LBL-24593
Preprint

Lawrence Berkeley Laboratory
UNIVERSITY OF CALIFORNIA

APPLIED SCIENCE DIVISION

Submitted to the Journal of Climate and Applied Meteorology

Vegetation Canopy Micro-Climate: A Field-Project in Davis, California

H. Taha, H. Akbari, and A. Rosenfeld

July 1989

APPLIED SCIENCE DIVISION

LOAN COPY
Circulates
for 2 weeks
Bldg. 50 Library.
LBL-24593
Copy 2

Prepared for the U.S. Department of Energy under Contract Number DE-AC03-76SF00098.

DISCLAIMER

This document was prepared as an account of work sponsored by the United States Government. While this document is believed to contain correct information, neither the United States Government nor any agency thereof, nor the Regents of the University of California, nor any of their employees, makes any warranty, express or implied, or assumes any legal responsibility for the accuracy, completeness, or usefulness of any information, apparatus, product, or process disclosed, or represents that its use would not infringe privately owned rights. Reference herein to any specific commercial product, process, or service by its trade name, trademark, manufacturer, or otherwise, does not necessarily constitute or imply its endorsement, recommendation, or favoring by the United States Government or any agency thereof, or the Regents of the University of California. The views and opinions of authors expressed herein do not necessarily state or reflect those of the United States Government or any agency thereof or the Regents of the University of California.

LBL-24593

VEGETATION CANOPY MICRO-CLIMATE: A FIELD-PROJECT IN DAVIS, CALIFORNIA.

Haider Taha, Hashem Akbari, and Arthur Rosenfeld

Applied Science Division
Lawrence Berkeley Laboratory
University of California
Berkeley CA 94720

July 1989

This work was supported by a grant from the University-Wide Energy Research Group of the University of California and the Assistant Secretary for Conservation and Renewable Energy, Office of Building and Community System, Building System Division of the U.S. Department of Energy under contract No. DE-AC0376SF00098.

ABSTRACT.

Dry-bulb temperature, dew-point, wind speed, and wind direction were measured in and around an isolated vegetative canopy (orchard) in Davis CA. These meteorological elements were measured 1.5 m above ground along a transect of seven weather stations set up across the canopy and upwind/downwind open fields.

The meteorological variables were recorded for two weeks in October 1986 so we could analyze their spatial and temporal fluctuations as well as their diurnal cycles. Our objective was to quantify the impact of the canopy on microclimate. The results indicate significant nocturnal heat islands and daytime oases, especially in clear weather. Inside the canopy within five meters of its upwind edge, daytime temperature dropped by as much as 4.5 °C, and the nighttime temperature rose by 1 °C. Deeper into the canopy and downwind, the daytime drop in temperature reached 6 °C, and the nighttime increase reached 2 °C. Data from this project were used to in conjunction with our models of evapotranspiration, shading, and wind-shielding effects of vegetative canopies.

Keywords: canopy, characteristic distance, cooling rate, evapotranspiration, heat island, heating rate, oasis effect, sky view factor, thermal mass, trees, microclimate.

INTRODUCTION.

Our objective in this project was to use field measurements to better understand the micro-climate within and around tree stands and improve our vegetation energy and moisture balance models. The ultimate goal of this work was to evaluate the potential of trees for reducing building cooling energy and peak power in hot climates, particularly in locations with significant summer heat islands. This paper describes the work with an isolated tree canopy in Davis CA.

It is known that urban heat islands in hot climates can significantly increase summer cooling loads in buildings, and particularly the envelope-dominated ones. Akbari et al. [1986], Huang et al. [1987], and Taha et al. [1988] investigated several strategies to alleviate heat islands. They found that one promising strategy, the implementation of vegetative canopies and shelter belts, can save up to 30% on peak cooling power and up to 50% on cooling energy. Vegetative canopies can also improve the micro-climate, particularly in urban areas. This field-project analyzes micro-meteorological conditions upwind, downwind, and within an isolated orchard in Davis, California. In particular, the effects of trees on ambient dry-bulb temperature, dew-point, and wind speed are studied.

In this paper, we first describe the site, equipment, and method of data collection for our project. We then briefly mention the calibration procedures and equipment problems encountered in the field. Finally we discuss the results in the main body of the paper, which is broken down into several sections. Temperature, dew-point, wind speed, and wind direction data are first examined for the entire observational period. Afterwards, data are segregated according to day or night, and clear or overcast conditions. Furthermore, those hours when the wind blew parallel to the line (transect) of weather stations are considered separately. Spatial variations across the stations' transect and temporal fluctuations at each location are also presented.

SITE DESCRIPTION.

We selected a well-defined vegetative canopy (orchard) in Davis to investigate the effects of trees on the micrometeorological conditions within and around them. Initially, eleven automatic weather stations, labeled A through K, were set up across the site, with "A" as the northernmost station (Figure 1). At the time of the experiment, in October 1986, the canopy had a cover of 30% based on shadow-percentage calculations from field photographs. The canopy was slightly discontinuous in cover near the middle, where the ground and a weather station (G) were relatively more exposed to the sky.

This canopy and its surroundings were ideal for our objectives: the air blew from an upwind open field into the canopy, where it was modified, and then continued to blow onto the downwind open field, where it gradually returned to its original state after a certain characteristic distance. The canopy had dimensions of 307 m in the north-south direction and 150 m in the east-west direction. It was bounded by a farm road on the north and a stream lined with tall evergreen trees and bushes to the south. The canopy trees' crown and stem heights were 5 m and 2 m, respectively. The evergreen trees at the stream were

15-20 m high and formed a more significant obstacle to the wind. Their cover was greater than that of the canopy (~ 95%).

Empty fields to the north and south stretched over 2 kilometers away from the canopy. The empty southern field was of particular interest to us because it was downwind during daytime and, therefore, the location where we would expect to see the advected air cooled by the canopy's evaporative effect.

The orchard was watered five days prior to the start of our experiment and the soil was still muddy when our weather stations were set up. Such conditions were ideal for studying the effects of unrestricted (potential) evapotranspiration when unlimited amounts of water are available for release to the atmosphere. On the other hand, the fallowing north and south fields were perfectly dry.

We set our weather stations so that there were three on the northern and three on the southern fields and five within the canopy (Figure 1). There was one hygrometer on the north field, two on the southern field, and three within the orchard. The clear-weather prevailing wind direction was north to south during daytime and south to north at night, so we set up the weather stations on a north-south transect.

DURATION.

Data collection lasted 14 days, from October 12 to 25, 1986. Preparing, testing, and calibrating the equipment started early in August. Since the data-loggers were not designed for outdoor use, we planned for no longer than three weeks of data collection to avoid the possible October storms that move into the Central Valley of California. Additional time was spent to shelter the equipment and connect over a kilometer of wires to the main power outlet.

EQUIPMENT DESCRIPTION.

We measured the meteorological variables of interest at one level within the canopy, 1.5 m above ground surface with automatic monitoring weather stations consisting of the following components:

A. **Weather heads** (wind anemometers and vanes): plastic cup anemometers, type Weather Measure model W200-SD wind speed sensors and vanes model W200-WS wind direction sensors. The average wind speed threshold of the anemometers was 1.5 m s^{-1} according to field observations during dynamic calibration. When tested in a wind tunnel however, one of the anemometers showed a threshold between 2.5 and 3.5 m s^{-1}. The average response of the vanes to wind direction started at ~2 m s^{-1}.

B. **Dry-bulb temperature sensors**: AD590 semiconductor dry-bulb sensors, accurate to ±0.5 °C. They were placed in cylindrical PVC radiation shields facing north, or, when hygrometers were used, they were housed in aspirated plastic cylinders along with chilled mirrors and circuitry.

C. **Chilled-Mirror Hygrometers**: dew-point sensors Model General Eastern DEW-10, operating on optical depth basis. The chilled mirror and its circuitry were housed in an aspirated plastic cylinder

about 17 cm in diameter and 65 cm in height, equipped with an exhaust fan at its bottom.

D. **Conditioning boxes**: signal conversion boxes, that transferred information to the data loggers. They converted sensor output signals into voltages within 0-5 volts. They were also the source for 24 VAC to power the fans and the chilled mirrors.

E. **Data-loggers**: Energy Signature Monitors (ESM) each with 16 channels for data logging. These micro-processor-controlled data loggers wrote information on 24K EPROM data modules.

F. **EPROM data-modules**: Each module had a capacity of 24K. At each reading, 6 bytes were allocated for time and date, and 2 bytes were used for each variable entry.

For practical reasons, the data loggers and the conditioning boxes had to be placed close to the weather heads. This setup required over a kilometer of wires to power the weather stations and took four days to complete. Several site and hardware problems reduced the useful number of weather stations from 11 to 7. Only stations A, C, D, E, G, I, and J yielded reliable results and were therefore considered in this paper.

CALIBRATION.

We calibrated the weather stations at the Lawrence Berkeley Laboratory (LBL) in Berkeley and the Richmond Field Station (RFS) in Richmond CA. Static calibration involved adjusting the appropriate resistances in the conditioning boxes as follows: (1) wind direction output adjusted to 2.048 volts with wind vanes pointing due south, (2) wind speed output adjusted to 4.0 volts when 9.4 VAC input was applied, (3) dew-point channel resistance set to 200 Ω (0.8-4 volts corresponded to 0-50 °C dew-point), and (4) dry-bulb channel resistance set to 1000 Ω (output corresponded to 10 mv $°K^{-1}$).

Dynamic calibration was carried out at the RFS using two-days' worth of data (3-5 October 1986). Figures 2, 3, and 4 depict the calibration curves for the stations that ran properly in Davis. Station A was selected as the temperature and wind speed control station, because it was the northernmost upwind location during the day. Station J was the control station for dew-point. The calibration process resulted in the following regressions:

Calibrated temperature	R^2	Significance	Standard error
T_c=-26.3974+1.0839Ta,	0.9801	0.00	1.186
T_d=0.8359+0.9863Ta,	0.9216	0.00	1.836
T_e=-5.5565+1.0150Ta,	0.9801	0.00	0.996
T_g=-10.2309+1.0323Ta,	0.9604	0.00	1.497
T_i=-4.5535+1.0061Ta,	1.0000	0.00	0.451
T_j=-3.0485+1.0020Ta,	0.9801	0.00	0.716

The left side of each equation represents the dry-bulb temperature at the given stations (°K), and Ta is the temperature at control station A. Similarly, the following table gives the regressions for wind speed, where Va is wind speed (m s^{-1}) at control station A.

Calibrated Wind speed	R^2	Significance	Standard error
V_c=0.1007+1.4747Va,	0.9409	0.00	0.109
V_d=-0.0608+0.8877Va,	0.9409	0.00	0.060
V_e=-0.0538+0.9126Va,	0.9604	0.00	0.055
V_g=0.1238+1.6974Va,	0.8836	0.00	0.176
V_i=-0.0147+1.0283Va,	0.9801	0.00	0.050
V_j=0.1735+1.7970Va,	0.7569	0.00	0.280

Dew-point calibration data are given in the following table, normalized to the dew-point at station J (D_j).

Calibrated Dew Point	R^2	Significance	Standard error
D_b=0.43958+1.0082Dj	0.952	0.00	0.033
D_d=-1.378+1.1510Dj	0.784	0.00	0.090
D_f=0.15224+0.99142Dj	0.931	0.00	0.040
D_i=-0.18479+0.99622Dj	0.937	0.00	0.038

In this project, humidity data were scarce. All but two hygrometers yielded unreliable or no information at all. Therefore, aside from a brief discussion of dew-point temperature, only dry-bulb and wind speed results will be considered in detail in the following discussions.

POST-CALIBRATION.

Because the equipment was immediately needed by other researchers, we could not recalibrate the equipment at the end of the data collection period. This final check should not be missed in future similar projects, to make sure the equipment has not suffered from transport or other effects, and that serious data drift has not occurred.

RESULTS AND DISCUSSION.

Tables 1-3 summarize the overall meteorological conditions at each weather station for the period October 12 through 25, 1986, including day/night times and clear/overcast skies.

Table 1. Overall dry-bulb temperature (°C) for the labeled stations (n=288).

	A	C	D	E	G	I	J
T_{min}	2.6	1.8	2.0	2.9	3.3	1.8	1.8
T_{max}	28.3	28.0	24.8	25.5	25.5	25.5	29.0
T_{mean}	13.04	12.39	11.96	12.38	13.09	11.91	12.33
st.dev	6.149	6.310	5.678	5.357	5.718	6.019	6.147

Table 2. Overall wind speed (m s^{-1}) for the labeled stations (n=288). (Wind speed data from station E were not available.)

	A	C	D	E	G	I	J
V_{min}	0	0	0	N/A	0	0	0
V_{max}	8.5	7.4	5.7	N/A	1.8	2.8	4.6
V_{mean}	1.63	1.5	.718	N/A	.299	.365	1.403
st.dev	1.7	1.469	1.063	N/A	.351	.4639	.9557

Table 3. Overall dew-point data (°C) for the labeled stations (n=288). († Humidity data from station D were unreliable.)

	D	I	J
D_{min}	-4.2†	3.3	.5
D_{max}	30.7	15.8	15.7
D_{mean}	5.94	8.77	7.29
st.dev	7.389	2.72	.193

Overall temperature data are presented in Figure 5 and overall wind speed data in Figure 8. In these figures the horizontal line at y = 0 represents the conditions at control station A. Figure 5 shows that the temperature difference between stations A and C was small and somewhat uniform because both stations were in the same open northern field. In the canopy, the temperature depression increased, and a diurnal pattern took shape. The canopy was cooler during daytime and warmer at night (stations D,E,G). In the southern field, station I also showed this pattern, indicating an influence from the canopy. It was cooler at station I during the day, but not as warm at night, because of the high sky view factor. Station J somewhat reflected the uniform pattern of upwind station C, indicating a comparatively small canopy effect at that location. Station G showed some higher temperatures (+0.5 °C) than station A at midday. The reason was that station G was within a clearing in the canopy, where solar radiation reaching the ground increased the surface temperature and the reduced wind speeds resulted in heat build-up.

Wind speed (Figure 8) was similarly affected. At station C, there was only a slight difference from control station A, whereas at station D, wind speed was significantly lower and was further reduced at Station G. It is clear that station I was under the influence of the canopy: despite its location on the open southern field, it showed the same wind pattern as station G. At station J in the open field, the difference in wind speed decreased again. Station E is not shown because of missing data.

A. Temporal variations (individual stations).

The following discussion refers to Figures 11 and 12, which depict the overall temperature and wind speed profiles at the given weather stations. In Figure 11, clear and overcast conditions can be detected in the different amplitudes of temperature fluctuations. One can also see that open-field weather stations had a larger range of temperature fluctuation than canopy stations. This was caused by the larger atmospheric cooling and warming rates in the open fields than in the canopy.

Figure 12 indicates that wind speed peaked almost always at 16:00 hours and reached a minimum at 7:00 hours in clear conditions. During cyclonic weather, wind speed almost invariably peaked at 15:00 hours and reached its lowest at 3:00 hours. All stations, whether within or outside the canopy, peaked at the same time. One can recognize in Figure 12 a typical wind speed pattern that is in phase with the temperature pattern. The similarity in phase is an indication of the effect of stronger convective mixing during the day. Wind speed reduction within and near the canopy is also evident (stations D,G, and I).

Wind direction in the open fields was relatively more predictable (especially during clear weather) than within the canopy, where the pattern was mostly erratic. That erratic pattern was partly due to the wind vanes' sensitivity threshold (which causes the vanes to point at different directions at low wind speeds) and partly because of wind redirection within the canopy. The prevailing wind direction in open fields was mainly from north during the day, and from south during evening and night hours.

Dew-point temperature is shown in Figure 13 for stations I and J. One can see that the dew-point at station I was the same as at J every day from 8 am to 4 pm, and was higher at other times. This indicates that station I was affected by the stream's and canopy's evaporative effects at all times and, despite the wind's reversal at night, station I was apparently still affected by the stream. During daytime, the fact that the dew-point was the same at both I and J suggests that there was no downwind moisture migration. But the lower temperatures at station I suggest that there was cool air advection from the canopy, however.

Heating and cooling rates.

The development of a heat island or oasis depends on the difference in atmospheric cooling and heating rates, respectively, among different sites. In the case of our orchard, the differential in cooling and heating was a result of different sky view factors and levels of wind-shielding between the canopy and the open fields (note that thermal mass difference was negligible). The following tables present the differences in atmospheric heating and cooling rates between the orchard and the open fields. In Tables 4 through 7 the cooling rates have been computed for the interval 16:00-7:00 hours, and the heating rates for 7:00-16:00 hours.

Table 4. Cooling and warming rates (c,w) in °C hr^{-1}, for the **open** site stations (outside the canopy), on **clear** days (12-15 October).

station	A		C		I		J		means	
	c	w	c	w	c	w	c	w	c	w
Oct. 12	-1.25	N/A	-1.32	N/A	-1.16	N/A	-1.15	N/A	-1.22	N/A
Oct. 13	-1.26	+2.25	-1.30	+2.32	-1.18	+2.15	-1.14	+2.16	-1.22	+2.22
Oct. 14	-1.46	+2.36	-1.57	+2.52	-1.36	+2.14	-1.40	+2.17	-1.44	+2.29
Oct. 15	-1.62	+2.53	-1.63	+2.68	-1.45	+2.30	-1.70	+2.61	-1.60	+2.53

Table 5. Cooling and warming rates (c,w) in ° Chr^{-1}, for the stations **within the canopy**, on **clear** days (12-15 October).

station	D		E		G		means	
	c	w	c	w	c	w	c	w
Oct. 12	-1.03	N/A	-0.98	N/A	-1.02	N/A	-1.01	N/A
Oct. 13	-1.12	+2.02	-1.07	+1.84	-1.04	+1.97	-1.07	+1.94
Oct. 14	-1.26	+1.98	-1.28	+1.98	-1.23	+1.90	-1.25	+1.95
Oct. 15	-1.32	+2.07	-1.36	+2.17	-1.35	+2.07	-1.34	+2.10

We can see that the canopy's cooling and warming rates were always smaller than the corresponding rates in the open sites. In other words, the daily range of temperature fluctuation within the canopy was damped. In the following table the canopy's cooling and warming rates are compared to the corresponding rates in the open fields. The numbers represent the ratios of the canopy's mean rates to the open fields' mean rates.

clear conditions		
	cooling ratio	warming ratio
Oct. 12	0.82	N/A
Oct. 13	0.87	0.87
Oct. 14	0.86	0.85
Oct. 15	0.83	0.83

One can see that the ratios were close to constant. Tables 4 and 5 are recast as Tables 6 and 7 for overcast conditions, keeping in mind the different timing of the high and low temperatures.

Table 6. Cooling and warming rates (c,w) in °C hr^{-1}, for the **open** site stations (outside the canopy), on **cloudy** days (16-19 October).

station	A		C		I		J		means	
	c	w	c	w	c	w	c	w	c	w
Oct. 16	-0.90	N/A	-0.95	N/A	-1.02	N/A	-1.13	N/A	-1.00	N/A
Oct. 17	-1.19	+0.94	-1.23	+0.99	-1.21	+1.05	-1.24	+1.12	-1.21	+1.02
Oct. 18	-0.77	+1.21	-0.79	+1.23	-0.87	+1.25	-0.82	+1.29	-0.81	+1.24
Oct. 19	N/A	+0.94	N/A	+0.97	N/A	+1.04	N/A	+0.96	N/A	+0.97

Table 7. Cooling and warming rates (c,w) in °C hr^{-1}, for the stations **within the canopy**, on **cloudy** days (16-19 October).

station	D		E		G		means	
	c	w	c	w	c	w	c	w
Oct. 16	-0.95	N/A	-0.88	N/A	-1.00	N/A	-0.94	N/A
Oct. 17	-1.20	+1.00	-1.08	+0.87	-1.11	+1.00	-1.13	+0.95
Oct. 18	-0.95	+1.35	-0.78	+1.17	-0.70	+1.13	-0.81	+1.21
Oct. 19	N/A	+1.00	N/A	+0.90	N/A	+0.85	N/A	+0.91

One can see that there was relatively less contrast between the canopy and the open fields in cloudy weather, as shown in the following table:

overcast conditions		
	cooling ratio	warming ratio
Oct. 16	0.94	N/A
Oct. 17	0.93	0.93
Oct. 18	1.00	0.97
Oct. 19	N/A	0.93

B. Oases and Heat Islands.

Figures 6 and 7 show that within the canopy (stations E and G), a well-defined heat island developed during evening and night hours, and that an oasis replaced it during the day. This is particularly true in clear weather (Figure 6) but still observable during overcast conditions (Figure 7). Heat islands and oases intensify in clear and calm conditions.

A typical heat island (or oasis) in the canopy stations G and E was 1.5-2 °C during clear weather (Figure 6), and 0.7-1.5 °C, under cloudy conditions (Figure 7). Oases resulted because of evapotranspiration and shading, whereas heat islands resulted mainly because of the reduced sky view factor (SVF=~60%) in the canopy. In clear conditions (Figure 6), stations D and I had an oasis because they were affected by the canopy's evaporative cooling, but they had no night time heat islands, because their sky view factors were large. In overcast conditions, the oasis effect was also reduced at both locations.

Figures 6 and 7 show that oases and heat islands occurred periodically with the same order of magnitude. An ideal heat island in the canopy is seen on clear days 1 through 4 (13 th through 16th of October 1986), with temperatures about 1.5 °C higher than at station A on the average (Figure 6). The heat island occurred during evening through early morning hours, between 19:00 and 8:00. On the other hand, the oasis effect occurred with an average 2 °C lower than at control station A, between 8:00 and 18:00 hrs. Instantaneous temperatures could be lower (-6 °C) or higher (+2 °C) than these average values.

The coolest station, on the average, was not within the canopy but just south of the stream, that is station I (see Figure 6). This can be explained by noting the prevailing wind direction. During the day, station I was under the effect of cool air advection from the canopy (north). That air was cooled by the orchard's evapotranspiration and contact with the orchard's cold soil. At night, on the other hand, that station was influenced by wind from the open field (south) whose soil was cooled by long wave radiation to the unobstructed, clear sky. Therefore, station I was generally cooler all the times. During clear weather the temperature at station I was as much as 6 °C lower than at A and was also lower than at other stations within the canopy. Its temperature reached that of station A only briefly at noontime.

Figure 14 represents the temperature profile for the entire site at hours when the wind direction was parallel to the weather stations' transect from north to south. There were only eight such hours out of the 336 hours of data collection. These hours' data are used to approximate the characteristic distances for this canopy. Each hour is represented by a single line in Figure 14. One can see that the dry-bulb temperature dropped sharply within the first few meters inside the canopy (through station E), but regressed back, at station G, to the same temperature of station A, because G is in a clearing. The excessive drop in temperature at station I can also be seen.

Table 8 summarizes the drop in temperature at the first two stations within the canopy at the same hours as in Figure 14 and along the wind path. This table shows that the greatest effect of the canopy occurred within the first five meters from the leading edge. Additional canopy depth was not as effective in lowering the temperature as the first few meters inside the canopy.

Table 8. Dry-bulb temperature drop (difference from temperature at control station A) at two distances within the canopy, downwind from the upwind edge.

day-hr	distance downwind in canopy	
	5m (D)	75m (E)
13-14	-1.2	-1.8
15-13	-1.8	-2
19-11	-.5	-1.1
19-16	-1.3	-1.4
21-13	-1.9	-1.9
22-15	-.7	-1.2
22-16	-2.1	-1.5
22-17	-2	-1.8

C. Spatial Characteristics.

Figures 16 through 23 depict the spatial variations in dry-bulb temperature at 00,03,06,09,12,15,18, and 21 hrs for all days in the observational period. One can see the progression of both heat islands and oases. In Figure 16 at midnight, there was a heat island within the canopy at stations D,E, and G, while

station I was generally the coolest. In this figure, the wind was blowing from the right side (from south) and is probably the reason that the stations in the northern field (at left) were relatively warmer than those in the southern one (at right). These stations were sheltered from the wind by the canopy. That the lowest temperature in the north field occurred sometimes at station C, however, was possibly a result of changing wind direction. At 3:00 hr, (Figure 17), the same pattern prevailed although at lower absolute temperatures. The average intensity of the heat island remained similar. Note that throughout this time, station I was generally the coolest.

At 6:00 hrs (Figure 18) the well-defined heat island in the canopy disappeared and was replaced by an oasis in Figures 19 and 20 at 9:00 and 12:00 hrs respectively (stations D,E, and G). At that time, station D, rather than I, was the coolest. Station G was warmer because it was within the clearing. At 15:00 hrs (Figure 21) the oasis leveled off; there was less contrast between the temperatures inside and outside the canopy. Yet, temperatures were still higher upwind (left of page) than downwind of the canopy because of advected cool air to the downwind field (right side in figure). At 18:00 hrs (Figure 22), the heat island was recreated and the contrast in temperature between the canopy and open increased at 21:00 hrs (Figure 23). The diurnal cycle was thus completed.

Clear versus overcast conditions.

This section discusses the effects of cyclonic weather and cloudiness on temperature and wind speed. In Figure 11, one can see that during cyclonic weather, the diurnal dry-bulb temperature range was damped by as much as 17.3 °C in the open sites, and as much as 12.5 °C in the canopy. In clear weather, the open fields reached a maximum dry-bulb temperature of 28.3 °C, and a minimum of 5 °C (ΔT=23.3 °C); in overcast conditions, these temperatures were 16 and 10 °C respectively (ΔT=6 °C). In the canopy, the clear-weather range was 26 °C to 7.5 °C (ΔT=18.5 °C), and the cloudy-weather range was 17 °C to 11 °C (ΔT=6 °C).

The effect of the cyclonic system on wind speed can be seen in Figure 12. In the open fields (station A), the highest wind speed during cyclonic weather was 8.5 m s^{-1} while in anticyclonic or neutral conditions, the highest was about 2.6 m s^{-1} (ΔV=6 m s^{-1}). In the canopy (station G), the typical highest speed in cyclonic weather was 1.8 m s^{-1}, and in anticyclonic weather it was 0.7 m s^{-1} (ΔV=1.1 m s^{-1}). The sharp spikes in wind speed, especially near the center of the graphs (Figure 12), were due to low-pressure system's winds and were not caused by micro-scale effects. The cyclonic system also overrode the prevailing wind direction, so that instead of the usual northerly and southerly winds, there were west and south-west winds.

Both nocturnal heat islands and daytime oases were strongly affected by cloudiness. As mentioned earlier, there was an average ±2 °C difference from the open sites during clear weather. In overcast conditions, the difference was reduced to an average -1 °C; that is, there was no heat island effect during overcast conditions, but a constant, mild oasis. As seen in Figure 7, the sinusoidal pattern of temperature was

still observable in overcast conditions, but aside from a short time interval at stations E and G, the scatter was below the zero-line representing station A. This can be attributed to the effect of evapotranspiration from the soil-vegetation system. It is interesting to note that station I was no longer the coolest during overcast conditions (Figure 7) and that its temperature profile became more like those in the canopy and in the open sites. This pattern was also due to the change in wind direction caused by the cyclonic system.

Temperature and characteristic distances.

One of this paper's objectives was to identify the downwind, characteristic distances over which the temperature, humidity, and wind-shielding effects of the canopy could still be detected. Because of prevailing north-south winds during the day, the southern site was the location where characteristic distances should be measured.

In order to simplify the analysis of characteristic distances, we constructed two sample days. These days, one cloudy and one clear, were made up of 24 mean hours each. They are shown in Table 9 and in Figures 24 and 25. In these figures, all stations are shown for two time snapshots (3 am and 3 pm) during clear and overcast conditions. Table 9 gives data for sample days at stations I and J on the southern field. During the clear sample day, station I was always cooler than station J, except for the interval 9:00 to 13:00, inclusive (Table 9). During the cloudy sample day, station I was cooler than J from 12:00 to 23:00 inclusive, and the temperature depression was smaller.

Table 9. Dry-bulb temperature profiles for stations J and I, on the sample clear and cloudy days.

	clear sample day			cloudy sample day		
time	I	J	Δ(i-j)	I	J	Δ(i-j)
0	8.2	8.7	-0.5	7.3	7.3	0.0
1	7.6	7.9	-0.3	6.6	6.5	0.1
2	7.2	7.5	-0.3	6.3	6.0	0.3
3	6.6	6.8	-0.2	6.4	6.0	0.4
4	6.0	6.3	-0.3	6.0	6.0	0.0
5	5.3	6.1	-0.8	5.9	5.8	0.1
6	5.0	5.8	-0.8	5.4	5.3	0.1
7	5.0	6.0	-1.0	6.1	5.8	0.3
8	7.9	8.0	-0.1	8.1	7.5	0.6
9	12.7	12.2	0.5	11.3	10.7	0.6
10	16.7	16.2	0.5	13.7	13.5	0.2
11	19.6	19.2	0.4	15.4	15.3	0.1
12	22.0	21.8	0.2	17.8	18.1	-0.3
13	23.6	23.6	0.0	18.5	18.7	-0.2
14	24.4	24.9	-0.5	19.0	19.2	-0.2
15	25.0	25.7	-0.7	19.9	20.3	-0.4
16	24.8	26.7	**-1.9**	19.0	19.5	-0.5
17	22.7	25.1	**-2.4**	17.1	17.7	-0.6
18	17.6	21.3	**-3.7**	14.7	15.4	-0.7
19	14.7	15.8	**-1.1**	12.2	12.7	-0.5
20	13.1	13.7	-0.6	11.1	11.8	-0.7
21	10.8	11.8	-1.0	10.6	11.1	-0.5
22	9.9	10.5	-0.6	9.8	10.1	-0.3
23	8.7	9.4	-0.7	9.3	9.6	-0.3

The difference in temperature between stations I and J was greater in the clear sample day, as shown in boldface in Table 9. The largest differences occurred between 16:00 and 19:00 hrs because evapotranspiration increases with higher ambient temperature and radiation. The table shows that station I was influenced by the canopy's cooling effect during the day.

Since station I was 12 meters away from the canopy's downwind edge, a lower bound of 12 meters can be assigned for the temperature characteristic distance of this orchard. Station J was 100 meters south of I, that is at 112 meters from the edge of the canopy. To determine whether this station's temperature was affected by the orchard, its data were compared to that of station A in the northern field, as shown in Table 10.

Table 10. Upwind/downwind comparison of temperature, on sample days.

	clear day		cloudy day	
hour	Δa-i	Δa-j	Δa-i	Δa-j
0	1.1	0.6	1.3	1.3
1	1.4	0.5	1.2	1.2
2	1.4	0.4	1.6	1.9
3	1.0	0.8	1.5	1.9
4	0.8	0.5	1.5	1.5
5	0.7	0.1	1.3	1.4
6	0.7	-0.1	1.0	1.1
7	0.4	-0.6	1.0	1.3
8	0.5	0.4	0.6	1.2
9	0.1	0.6	0.4	1.0
10	-0.3	0.2	0.4	0.6
11	-0.5	-0.1	0.6	0.7
12	-0.3	-0.1	0.5	0.2
13	0.2	0.2	0.8	0.6
14	1.0	0.5	0.8	0.6
15	**1.4**	0.7	0.8	0.4
16	**2.1**	0.2	1.1	0.6
17	**3.4**	1.0	1.7	1.1
18	**5.4**	1.7	**2.1**	1.4
19	**2.0**	0.9	**2.0**	1.5
20	1.6	1.0	**2.0**	1.3
21	**2.1**	1.1	1.7	1.2
22	1.3	0.7	1.6	1.3
23	1.6	0.9	1.4	1.1

One can see that in clear weather, the largest differences from station A (shown in bold) were greater at station I than station J, indicating a stronger canopy effect at I. We can also see that station J was cooler than A especially after 15:00 hours, indicating that it was also within the characteristic distance of the canopy at that time. In overcast conditions, the difference in temperature between stations I and J was damped, as seen on the right side of Table 9. The largest temperature difference was only 0.7 °C in late afternoon and evening, compared to 3.7 °C in clear conditions.

With these conditions in mind, we can conclude that this canopy had a temperature characteristic distance between 12 and 112 meters (one to five times the height of the evergreen trees at the south end of the canopy) most of the time. Also, there were times when station J was influenced by the canopy, meaning that the temperature characteristic distance exceeded 100 meters. Just exactly where the canopy's effect ended could not be determined with only two downwind stations 100 meters apart. In the future, we should set all our weather stations downwind of the canopy, within 100 meters of its trailing edge to find the exact location and time fluctuation of the characteristic distance for temperature.

D.Wind pattern and characteristic distances.

It is difficult to generalize about wind direction within and immediately surrounding the canopy. However, there were some observable patterns, particularly in the open fields. For the purpose of this discussion, we examined data from the first six days of the experiment (three clear and three overcast).

It is particularly interesting to discuss the 18th of October, which was the windiest day of observation (Figure 12, middle spikes). The consistency in wind direction on that day was remarkable. With the exception of station I, all others had a consistent westerly wind. Station I had a more northwesterly component, probably resulting from local turbulence caused by the tall trees at the southern and western edges of the canopy. Otherwise, the consistent west wind was an indication of the strong effect of the cyclonic system during that day. The consistent wind direction allowed us to verify the characteristic distance through all hours. Table 11 represents the wind speed data for that day and can be thought of as a north-south section across the site with north at the left side of the page. Station E was dropped because its wind speed sensor was faulty.

Table 11. Wind speed m s^{-1}, on October 18th, 1986.

hr	A	C	D	G	I	J
0	1.0	1.0	0.2	0.1	0.1	0.8
1	1.5	1.5	0.6	0.1	0.1	0.8
2	1.8	1.8	1.0	0.1	0.1	0.9
3	1.6	1.4	0.6	0.1	0.1	0.9
4	3.5	3.1	1.8	0.5	0.2	1.7
5	2.3	2.0	1.4	0.3	0.1	1.4
6	1.2	1.2	0.3	0.1	0.1	0.6
7	3.8	3.3	2.0	0.8	0.2	2.1
8	3.0	2.7	1.6	0.4	0.2	1.7
9	5.8	5.2	3.4	1.2	0.6	3.2
10	7.0	6.3	4.3	1.5	0.8	3.6
11	8.5	7.4	5.7	1.8	1.0	4.6
12	8.3	7.3	5.4	1.8	1.1	4.6
13	8.2	7.3	5.6	1.8	1.1	4.6
14	8.0	7.0	5.4	1.7	1.1	4.4
15	7.6	6.8	4.9	1.6	0.9	3.9
16	7.4	6.6	5.1	1.6	0.9	4.1
17	6.8	5.8	4.5	1.4	0.7	3.8
18	4.2	3.6	3.2	0.8	0.3	2.4
19	2.5	2.3	1.3	0.2	0.1	1.4
20	2.7	2.4	1.3	0.4	0.1	1.3
21	3.6	3.2	1.8	0.9	0.2	1.9
22	3.8	3.3	1.8	0.9	0.2	2.1
23	4.1	3.5	2.1	0.9	0.3	2.3

The following notes refer to Table 11 (18th of October):

1. Comparison of wind speeds at stations I and J with those at stations A and C showed that the first two were within the wind characteristic distance of the canopy, although they were in open fields. The wind-shielding effect of the canopy was particularly strong at station I. Wind speed at J, although higher than at I, was always lower than that at stations A and C indicating that the wind characteristic distance for this canopy on that day was over 112 meters (greater than five times the height of the trees).

2. The station with the lowest wind speed on October 18 was not in the canopy but just south of it (station I). This was due to the sheltering effect of the tall trees just north and west of this weather station. Figure 15 shows the wind speed profile across the site at other hours when the wind blew parallel to the stations' line. As mentioned earlier, there were only eight such hours during the entire data collection period, and these are shown as eight curves in this figure. One can see that wind speed dropped quickly within the canopy (stations D and G) and regressed back to the undisturbed speed as it flowed onto the open field towards station J. Table 12 summarizes the drop in wind speed at two stations within the canopy. Compare it with Table 8 for temperature drop at these

same hours.

Table 12. Wind speed at two stations within the canopy, given as a ratio to wind speed at control station A.

day-hr	distance downwind in canopy	
	5m (D)	225m (G)
13-14	0.45	0.2
15-13	0.5	0.21
19-11	0.53	0.2
19-16	0.6	0.16
21-13	0.38	0.15
22-15	0.63	0.13
22-16	0.35	0.07
22-17	0.46	0.07

In Table 12, the 75m interval, corresponding to station E, was omitted because of anemometer malfunction at that location. As in the case of temperature (see Table 8), the effect of the first five meters of the canopy on wind speed was relatively much larger than that the effect of the next 220 meters.

Wind speed gradients from the upwind stations (north of the canopy) to the downwind ones (south of the canopy) were considerable. For example, at the highest wind, at 11:00, station A recorded 8.5 m s^{-1}, while station I recorded only 1.0 m s^{-1} (88% reduction). During the weakest winds, at 0:00 hr, station A had 1.0 m s^{-1} while station I had 0.1 m s^{-1} (90% reduction).

Figures 9 and 10 summarize the wind speed pattern for clear and overcast conditions, respectively. In clear weather, stations C and J had similar wind speed profiles to that of station A, because they were in open fields. The wind speed depression started at station D, as seen in Figure 9, with a wavy pattern that was in phase with that of temperature. The depression increased at station G, within the canopy, and at station I the pattern was still well defined, although that station was in an open field. Station I was the only open-field station to show significant wind speed influence from the canopy.

When a cyclonic system arrived, the same overall wind speed pattern prevailed, but the scatter increased because of higher absolute wind speeds in the open fields (Figure 10) and larger contrast between the open and canopy stations (D and G). Wind speed within the canopy was always lower than that at station A, or other open-site stations. Station J was shielded from the wind at high speeds, indicating that the wind characteristic distance increased with wind speed.

TEMPERATURE AND WIND-SPEED IMPACTS ON HEAT ISLANDS AND OASES.

In order to understand whether the lower temperature within the canopy was due to evapotranspiration alone or other effects as well, we correlated the drop in dry-bulb temperature to absolute temperature and to absolute wind speed at station A. Then we performed a bivariate analysis of temperature drop

versus both wind speed and absolute temperature. Because evapotranspiration increases directly with ambient temperature, a good correlation between T and ΔT would mean that the temperature depression was mainly caused by evaporative cooling effects. Also, the temperature depression is expected to vary inversely with wind speed.

Figure 26 depicts the regression curves for ΔT versus T for all hours. This includes clear and overcast conditions, day and night. The reference temperature used in these regressions was that of station A. One can see in this figure that the drop in temperature at stations C and J did not relate to absolute temperature, because all these stations were in open fields. At station I, on the other hand, the temperature scatter was too large above 10 °C, and it became impossible to identify any good correlation. Stations D, E, and G showed better correlations and indicated that the drop in temperature within the canopy was mainly due to evapotranspiration.

To further refine this analysis, the same regressions were repeated for clear weather only, including day and night hours (Figure 27). As expected, stations C, I, and J still did not correlate any better than before. On the other hand, stations D, E, and G showed better correlations, thus strengthening the indication that evapotranspiration from the soil-vegetation was a major factor in reducing the temperature within the canopy.

The regressions were repeated for daylight hours only, as seen in Figure 28, to determine whether there were any day- or nighttime dependence in temperature depression. There was no improvement in the correlations at stations D, E, and G, indicating no day- or nighttime dependence in temperature depression within the canopy. These regressions indicate, however, that evaporative cooling did not result mainly from foliage evapotranspiration (in which case it would have ceased or slowed at night) but mainly from soil moisture evaporation. In other words, the main source of moisture in the orchard, and therefore the most important factor in depressing the canopy's temperature was the soil and not the foliage. Recall that the canopy had only light cover (~ 30%) at that time. A denser foliage would have increased the proportion of evaporation from the foliage relative to that from the soil-vegetation system as a whole.

Figures 29 through 34 depict another way to understand temperature data. These figures show T versus ΔT segregated by day and night and clear and overcast conditions. Figure 29 indicates that there was not much difference in temperature between stations A and C at all times. The fact that station C was somewhat cooler can be attributed to its proximity to the canopy.

In Figure 30, the larger scatter indicates a significant difference in temperature at station D compared to that at A. At station D, the canopy was cooler during the day in both clear and overcast conditions. The large temperature depression seen at the right side of the figure occurred at times of highest temperatures coinciding with lowest wind speeds (during clear daylight hours in that observational period). Table 13 shows these times of coincidence:

Table 13. Coincident high temperatures and low wind speeds, where T_A is the temperature at station A.

day	hour	V	T_A
Oct. 13	18	1.0	22.6
Oct. 14	15	0.9	27.0
Oct. 14	16	0.5	27.4
Oct. 14	17	0.3	27.0
Oct. 14	18	0.1	23.7
Oct. 15	14	0.8	26.5
Oct. 15	16	0.5	28.3
Oct. 15	17	0.8	26.6
Oct. 15	18	0.1	22.8

The entries in Table 13 are arranged chronologically. Note that the temperature on the 15th of October at 16:00 hours (28.3 °C) was the highest recorded value during that observational period.

Figure 31 (station E) shows basically the same pattern as Figure 30, except that the magnitude of the nighttime heat island was greater. One can see that station E could be up to 2.2 °C warmer than the open sites at night. Station E was well sheltered and its low sky view factor was the main reason that it was warmer than station D (Figure 30), which had a higher sky view factor. The same explanations apply to station G as seen in Figure 32. The night-time temperature was slightly lower at station G than at E because the former was more open to the sky.

Figure 33 indicates that station I was one of the coolest on the average. There was no nocturnal heat island at that location, since station I was more open to the sky, but the advected air from the canopy kept it cooler, particularly in clear, daylight hours. Finally, Figure 34 describes station J, where both oases and heat islands were reduced, except for the times when this station was within the characteristic distance of the canopy.

In order to test the correlation between heat islands, oases, and actual wind speeds, we plotted these three phenomena against each other as in Figure 35. Clearly, the lower the wind speed at station A, the greater the heat island effect (positive scatter) and oasis effect (negative scatter). The minimal temperature depression occurred at wind speeds above 6 m s^{-1}. Another characteristic is the range of ΔT that was small in the open field stations and large in the canopy stations. Station J showed some temperature depression despite being in an open site. As explained earlier, this was due to the canopy's temperature characteristic distance effect. What is seen in Figure 35 can also be seen in Figures 29 through 34. The highest temperature depressions at the right sides of these figures occurred at times of low wind speeds.

WIND REDUCTION VERSUS WIND SPEED AND DIRECTION.

To further investigate the effects of the canopy on wind speed, we performed two additional tests: (1) wind speed reduction within the canopy versus absolute wind speed, and (2) wind speed reduction within the canopy versus wind direction. Figure 36 shows the first test. The y-axis represents the

depression in wind speed at the given stations (at all times) versus absolute wind speed at control station A. The correlation was good, especially in the middle of the canopy (station G). At the edges of the canopy (stations D and I) the correlation was still strong but some scatter was obvious, due to the shifting wind direction, which meant that each station was upwind (at the leading edge) at some times, and downwind (at the trailing edge) at others. Station C showed a shallow slope because it lied in the same open field as station A. On the other hand, station J showed some strong correlation, indicating that it was within the wind characteristic distance of the canopy as discussed earlier.

Figures 37 and 38 allow us to look at the decrease (deceleration) and increase (acceleration) in wind speed towards and away from the canopy, respectively. These figures include logarithmic fits to the data when the wind blew within 30° on either side of the stations' line. Thus, Figure 37 represents the hours when the wind blew from the north (± 30°), whereas Figure 38 shows the hours when it was coming from the opposite direction (south ± 30°).

One can see that there was a strong correlation between wind speed depression and horizontal distance. In a decelerating case (Figure 37), the horizontal distance was measured downwind from the leading edge of the canopy whereas in the accelerating case (Figure 38) it was measured from the downwind edge and outward. The regression equations and correlation coefficients are:

$$\frac{U_x}{U_a} = 0.76\, e^{-0.00528x} \qquad r^2 = 0.983 \quad (deceleration) \tag{1}$$

$$\frac{U_x}{U_j} = 1 - 0.49\, e^{-0.137x} \qquad r^2 = 0.902 \quad (acceleration) \tag{2}$$

where wind speed (m s^{-1}) at any distance (x) is correlated to wind speed at stations (a) or (j); x is the horizontal, downwind distance (m) from the starting point, i.e: the upwind edge of the canopy, in the decelerating case, and the downwind edge, in the accelerating case.

Equation (1) indicates that the upwind speed dropped to below that of the open fields (station A) at a point somewhere between stations A and C. As given in this particular regression, this point lied at 52 m upwind of station C, because the canopy deflected the wind upward at about that point. Equation (2) indicates that the downwind speed got back to that of the open fields at 45 meters from the downwind edge. The correlations are good, and we feel that these equations can be used in describing the wind behavior in and around a uniform canopy, such as the one in Davis.

CORRELATIONS WITH HEAT ISLAND AND OASIS EFFECTS.

We studied the correlations between the magnitudes of the heat islands, oases, absolute temperatures, and wind speeds. We found that the nighttime heat islands correlated better to temperature and wind speed than the daytime oases. The correlations for three canopy stations (D,E,G) and one open-field

station (I) are shown in tables below, where one can see that the latter station differs from the others in its dependence on temperature and wind. In the following tables, T and V respectively represent the temperature (°C) and wind speed (m s^{-1}) at control station A. The subscripts are used to denote other stations. For each equation, a coefficient of correlation is given with a significance value with respect to given variables.

NIGHT TIME

T_d-T = 0.016838 - 0.020764 T - 0.671089 V + 0.108067 V^2	r^2 = 0.6599	sig = 0.03T
T_e-T = 1.330847 - 0.063270 T - 1.162426 V + 0.207723 V^2	r^2 = 0.7914	sig = 0.00
T_g-T = 1.437209 - 0.038639 T - 1.119091 V + 0.233515 V^2	r^2 = 0.6593	sig = 0.00
T_i-T =-0.003957 - 0.132193 T - 0.200881 V + 0.039127 V^2	r^2 = 0.5885	sig = 0.14V^2,0.04V

T_d-T = -0.019529 - 1.416502 V + 0.616225 V^2 - 0.085730 V^3	r^2 = 0.6881	sig = 0.00
T_e-T = 1.016372 - 2.135706 V + 0.818662 V^2 - 0.100939 V^3	r^2 = 0.7695	sig = 0.00
T_g-T = 1.259224 - 1.803112 V + 0.671352 V^2 - 0.072712 V^3	r^2 = 0.6525	sig = 0.00
T_i-T = -0.832248 - 1.142896 V + 0.527303 V^2 - 0.076114 V^3	r^2 = 0.2733	sig = 0.04V^3

DAY TIME

T_d-T = -2.091156 - 0.030825 T + 0.515039 V - 0.033832 V^2	r^2 = 0.4485	sig = 0.00
T_e-T = -0.948869 - 0.052438 T + 0.176006 V - 0.011627 V^2	r^2 = 0.4192	sig = 0.13V^2
T_g-T = -0.789969 - 0.037055 T + 0.405912 V - 0.043835 V^2	r^2 = 0.3299	sig = 0.00
T_i-T = -0.750381 - 0.091788 T + 0.933425 V - 0.093946 V^2	r^2 = 0.3946	sig = 0.00

One can see that there was a good correlation (in canopy stations) between nighttime temperature depression and T, V, and V^2, as well as with V, V^2, and V^3. During the daytime, the correlation was best with T, V, and V^2, but was generally weaker than the night correlations. It is also clear that wind speed assumed a more important role in temperature depression than absolute temperature.

Based on this information, we propose the use of the following representative formulas to predict the temperature within a uniform canopy, when upwind open-field temperature and wind speed are known. These formulas were based on those of stations E and G only, in order to avoid possible edge effects at other stations.

nighttime, T and V known →	$\Delta T = 1.33 - 0.063\,T - 1.16\,V + 0.20\,V^2$	(r^2=0.80)	..... (3)
nighttime, V known →	$\Delta T = 1.02 - 2.14\,V + 0.82\,V^2 - 0.10\,V^3$	(r^2=0.77)	..... (4)
daytime, T and V known →	$\Delta T = -0.79 - 0.037\,T + 0.406\,V - 0.043\,V^2$	(r^2=0.33)	..... (5)

where ΔT is the temperature depression (heat island or oasis) in °C, within the canopy, and V and T are

the upwind wind speed (m s^{-1}) and temperature (°C), respectively. All these correlations are at statistical significance of zero. Equation (3) is for nighttime heat island prediction and yields realistic results in the domain of $0.5 \leq V \leq 1.5$ m s^{-1}. Within this domain, the balance point temperature† is ~ 6 °C. Similarly, Equation (4) has a domain of $0 \leq V \leq 1.0$ m s^{-1}, with a balance wind speed† of 0.6 m s^{-1}. Equation (5) is for daytime oasis prediction, and should be used with wind speeds higher than 2.5 m s^{-1}.

CONCLUSIONS.

In this project, we aimed at analyzing and quantifying the micro-meteorological conditions within and around a vegetative canopy in Davis, California, during a warm period in October 1986. Heat island and oasis effects were identified and quantified. The canopy was on the average 2 °C warmer than surrounding open areas at night, and 1.5 °C cooler during the day. The amplitude of temperature fluctuation (maximum minus minimum daily temperature) was damped in overcast conditions. In the open fields, the range was damped by as much as 17.3 °C, whereas in the canopy, the range was damped by as much as 12.5 °C.

Wind speed within the canopy was reduced in general, and its contrast with that of the open fields increased during cyclonic weather, when wind speeds in the open rose to 8.5 m s^{-1}. Under these conditions, wind speed within the canopy was only about 1.5 m s^{-1}. Temperature, humidity, and wind characteristic distances were suggested for that canopy, as evidenced from its influence on downwind stations in open fields. The canopy effect on downwind stations was seen in lowered temperatures, increased humidity, and lowered wind speeds. Characteristic distances for temperature fluctuated between 10 and 100 m downwind of the canopy into the open fields, whereas the characteristic distances for wind speed was generally greater than 100 m downwind of the canopy (over five times the height of the tall trees at the southern end of the orchard).

Our results indicate that the effects of the canopy were immediate: the first 5 meters inside the canopy from its upwind edge showed larger effects on temperature and wind speed than the next 200 meters or more. This preliminary field project was highly useful in identifying the relevant parameters to consider in future research of this kind.

ACKNOWLEDGEMENTS.

We would like to thank all the people who helped us in this project. At Lawrence Berkeley Laboratory they are: Rich Prill, Rich Szydlowski, Brian Smith, Ken Revzan, Bob Harvey, Les Lewicki, and Al Robb. In Davis we would like to thank Charles McGinn, Diane and Mark Tauzer, Gene Stiles, and Roth

†Balance point temperature (or wind speed) is the temperature (or wind speed), in the open fields, above which an oasis existed in this canopy and below which a heat island prevailed in the canopy.

Brothers. In the UC-Berkeley services department (DOFM) we are grateful to Rich Fahey.

This work was supported by a grant from the University-Wide Energy Research Group of the University of California at Berkeley, and the Assistant Secretary for Conservation and Renewable Energy, Office of Building and Community System, Building System Division of the U.S. Department of Energy, under contract DE-AC0376SF00098.

REFERENCES.

Akbari, H., Taha, H. Huang, J., and Rosenfeld, A. 1986. "Undoing Uncomfortable Summer Heat Islands Can Save Gigawatts of Peak Power", Proceedings of the ACEEE Summer Study on Energy Efficiency in Buildings, August 1986, Santa Cruz, California.

Huang, J., Akbari, H., Taha, H., and Rosenfeld A. 1987. "The Potential of Vegetation in Reducing Summer Cooling Loads in Residential Buildings", Journal of Climate and Applied Meteorology, Vol 26, No. 9, pp.1103-1116.

Taha, H., Akbari, H., Rosenfeld, A., and Huang, J. 1988. "Residential Cooling Loads and the Urban Heat Island: The Effects of Albedo". Building and Environment, Vol. 23,No. 4, pp. 271-283.

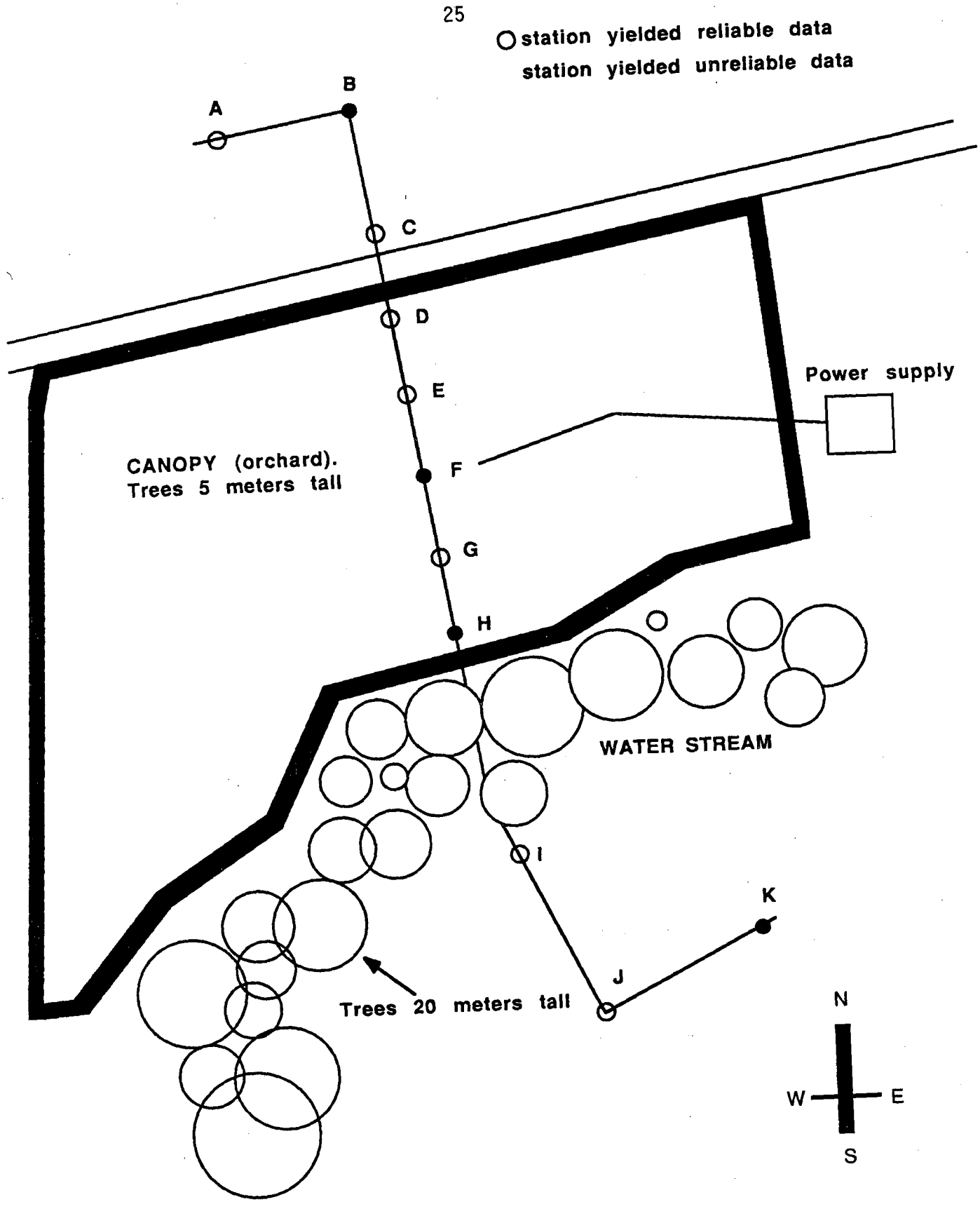

Figure 1. Site plan of the canopy (orchard) and the weather stations. Not to scale.

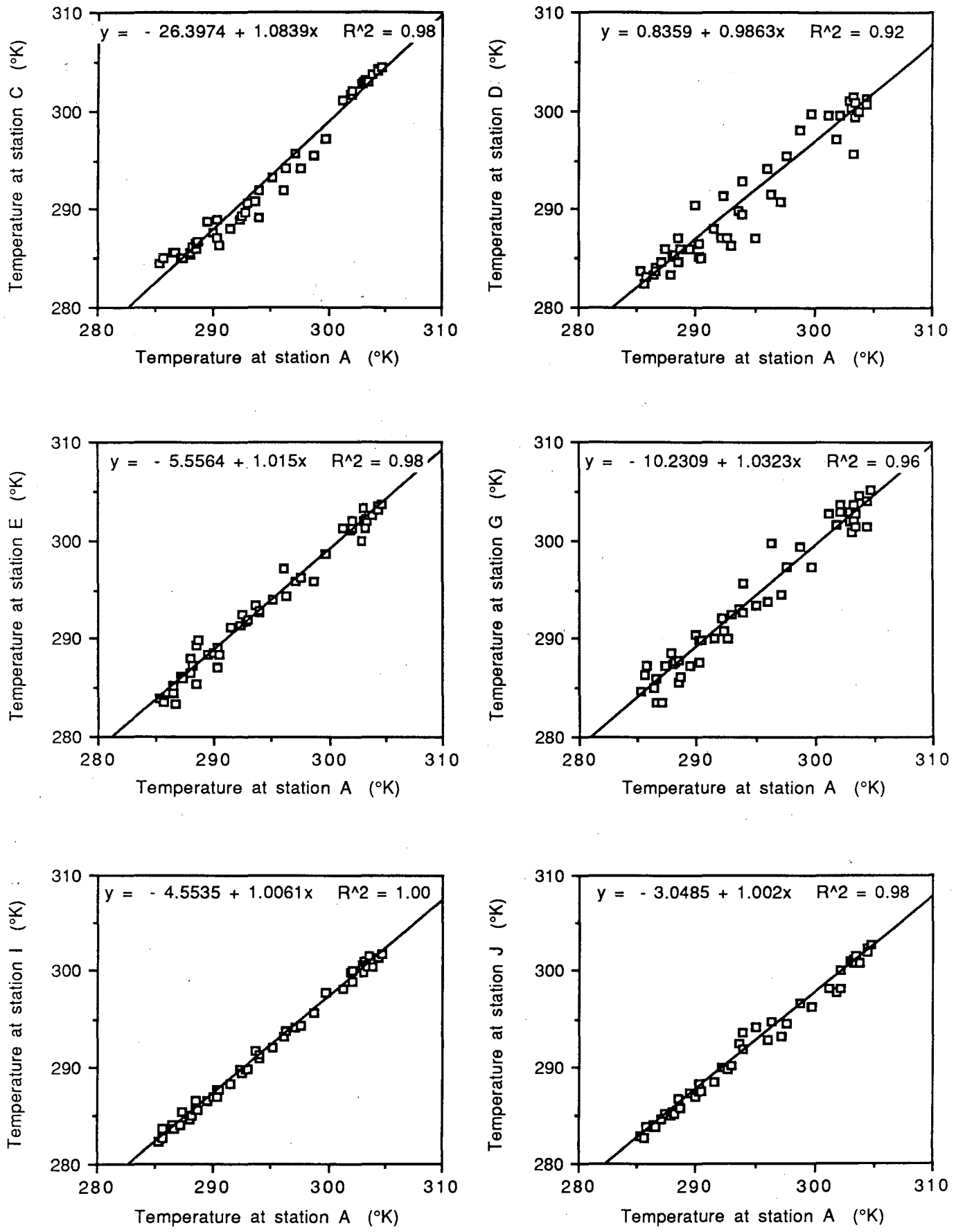

Figure 2. Temperature calibration regressions. Control station is location A.

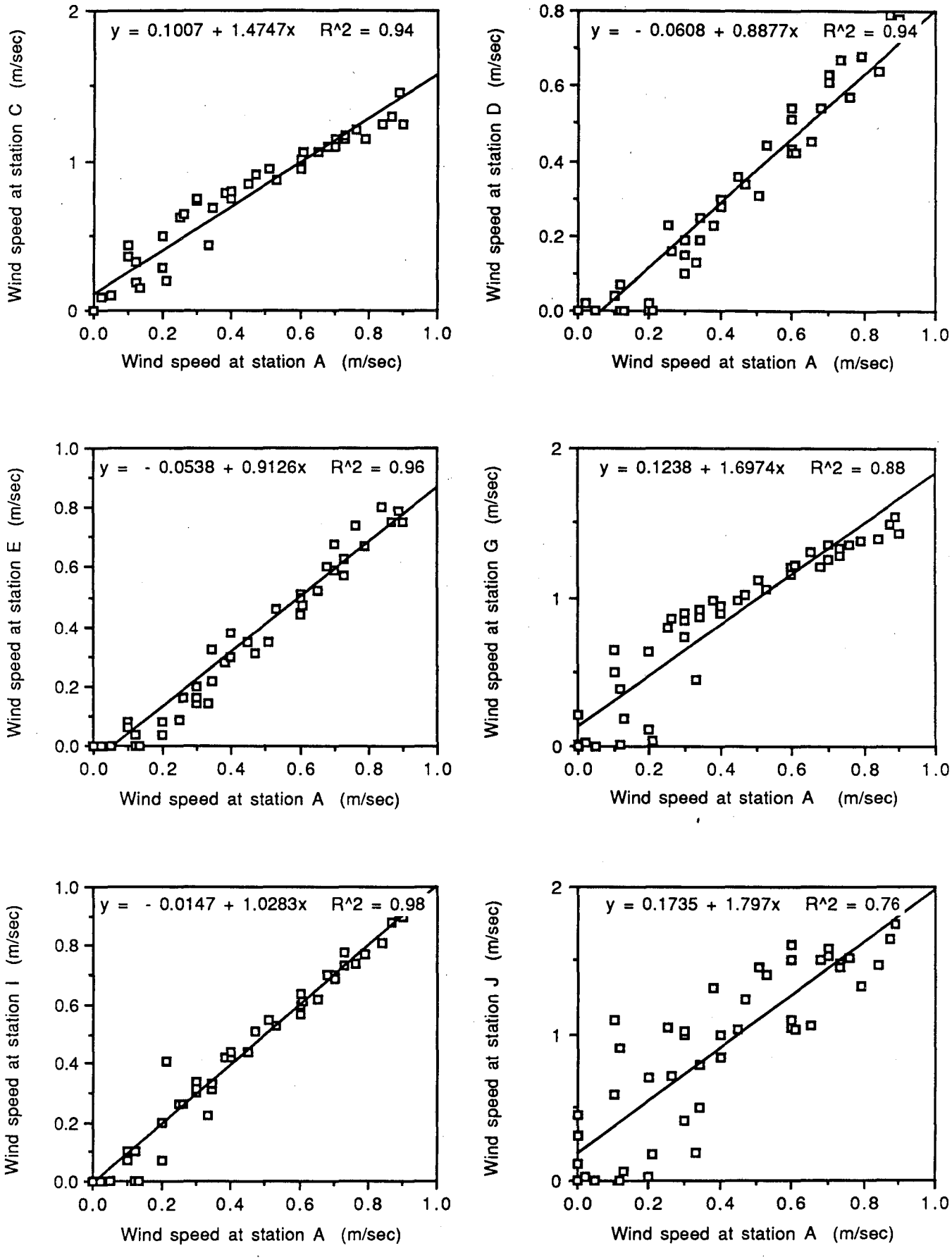

Figure 3. Wind speed calibration regressions. Control station is location A.

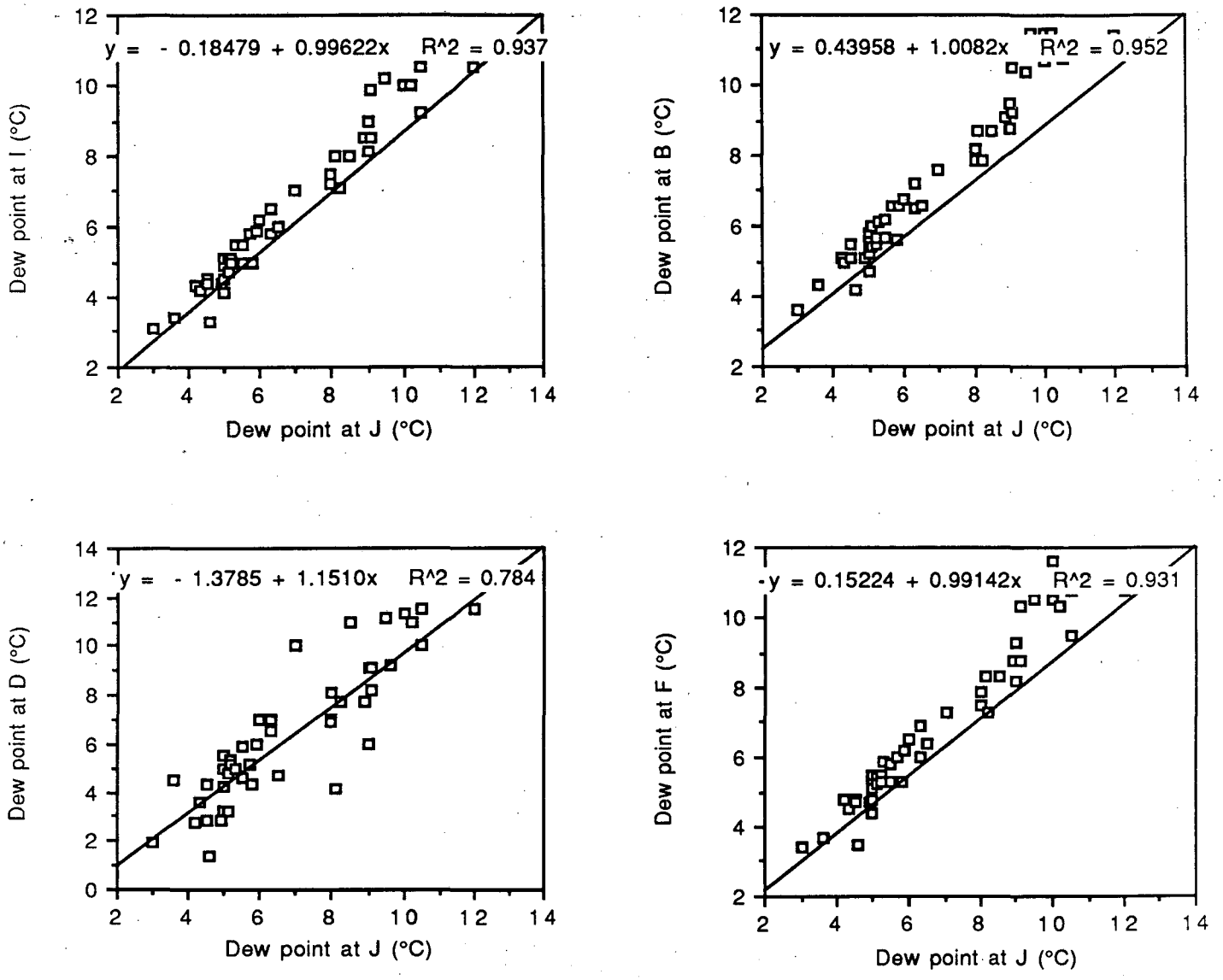

Figure 4. Dew-point calibration regressions. Control station is location J.

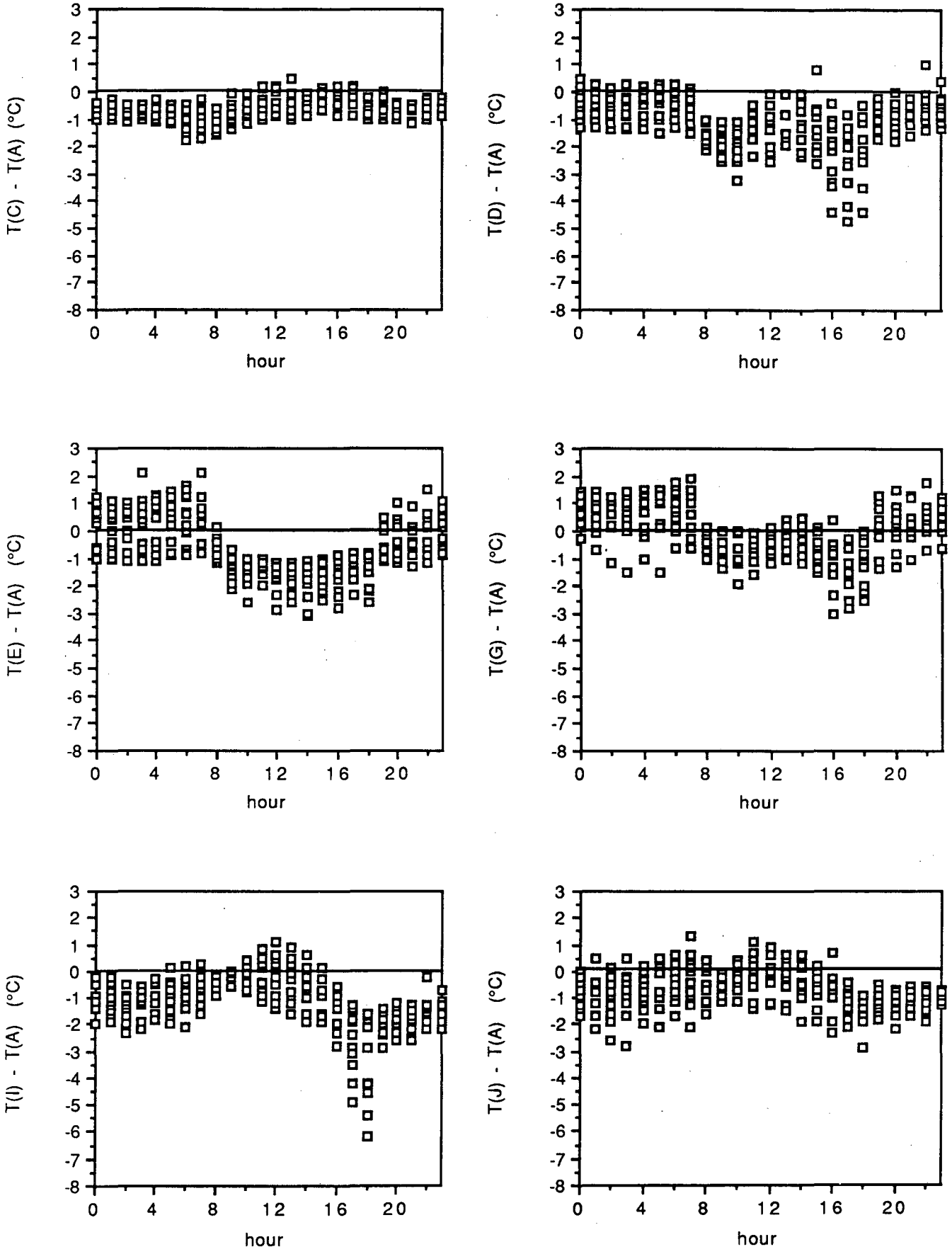

Figure 5. Temperature difference from station A (°C) for all 14 days. Includes day/night and clear/overcast conditions.

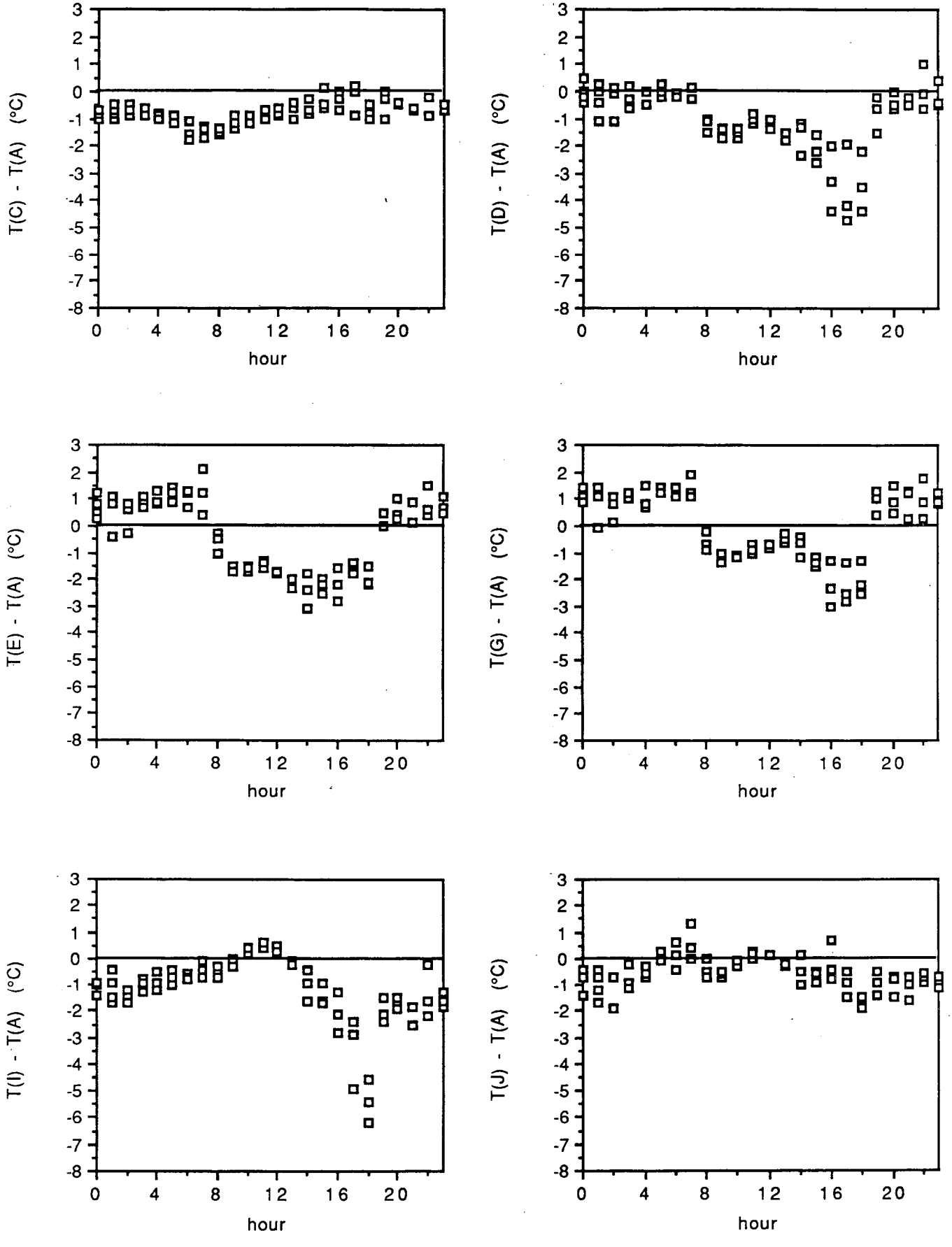

Figure 6. Clear day and night temperature difference from station A (°C) for 3 days.

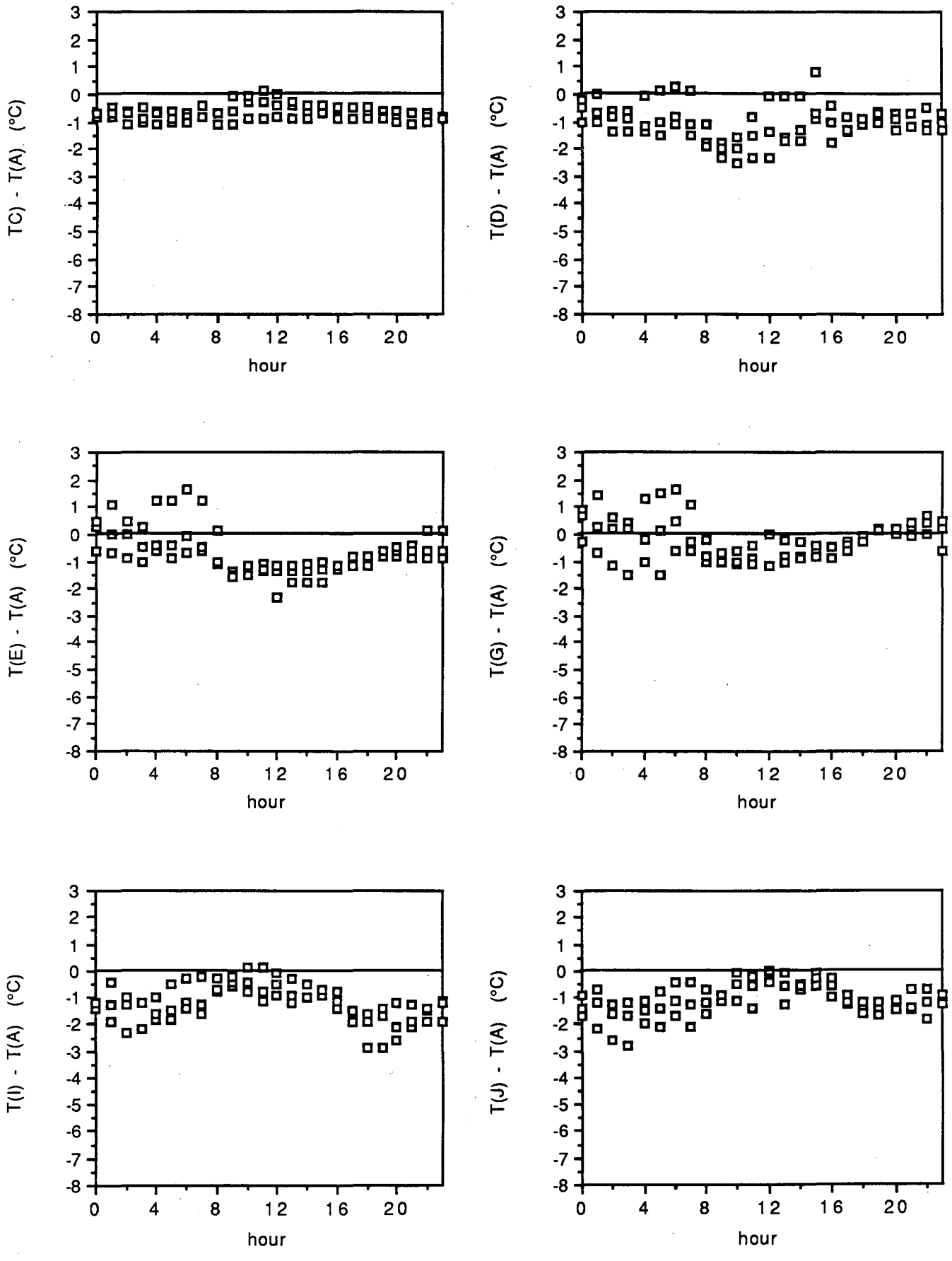

Figure 7. Overcast day and night temperature difference from station A (°C) for 3 days.

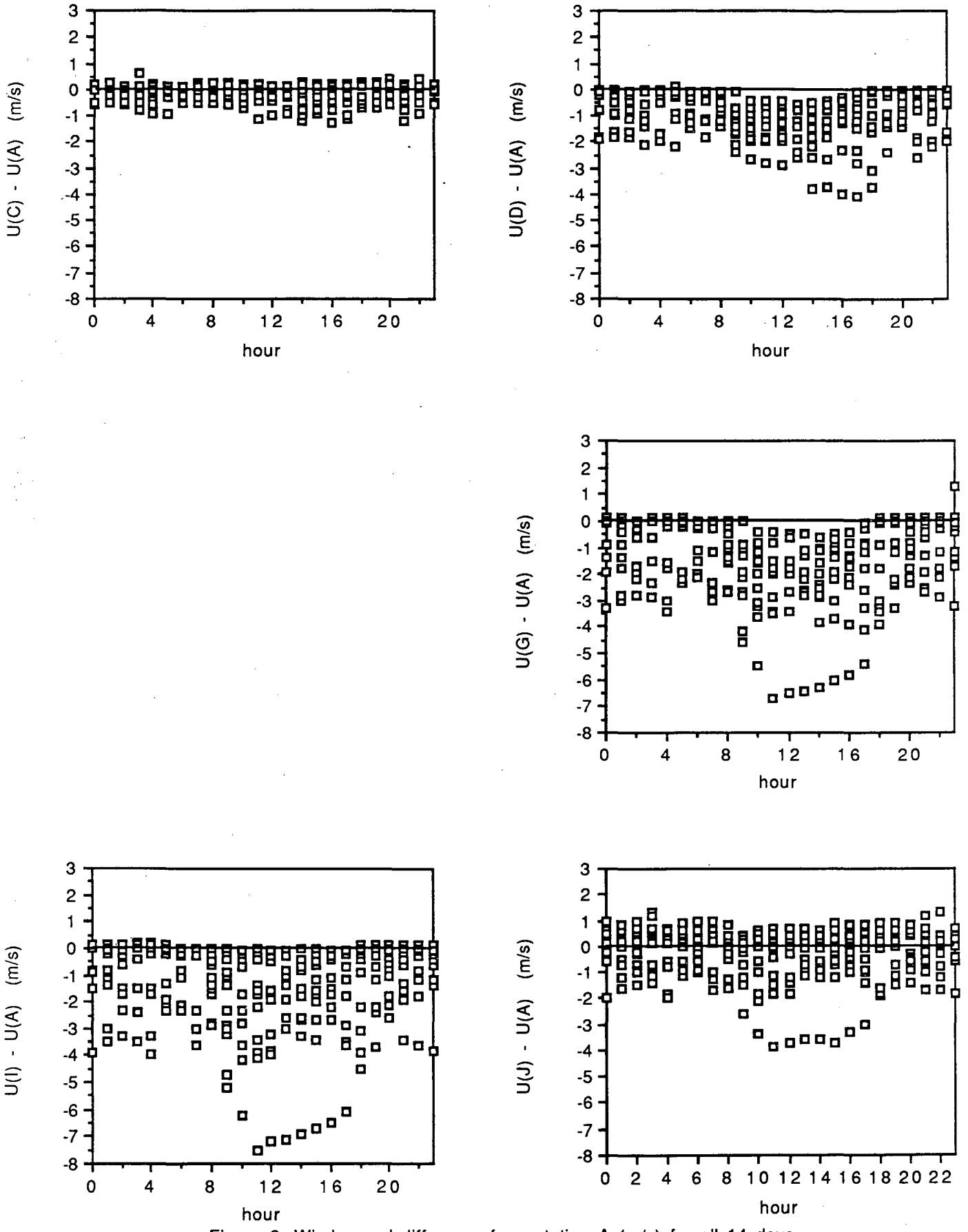

Figure 8. Wind speed difference from station A (m/s) for all 14 days. Includes day/night and clear/overcast conditions.

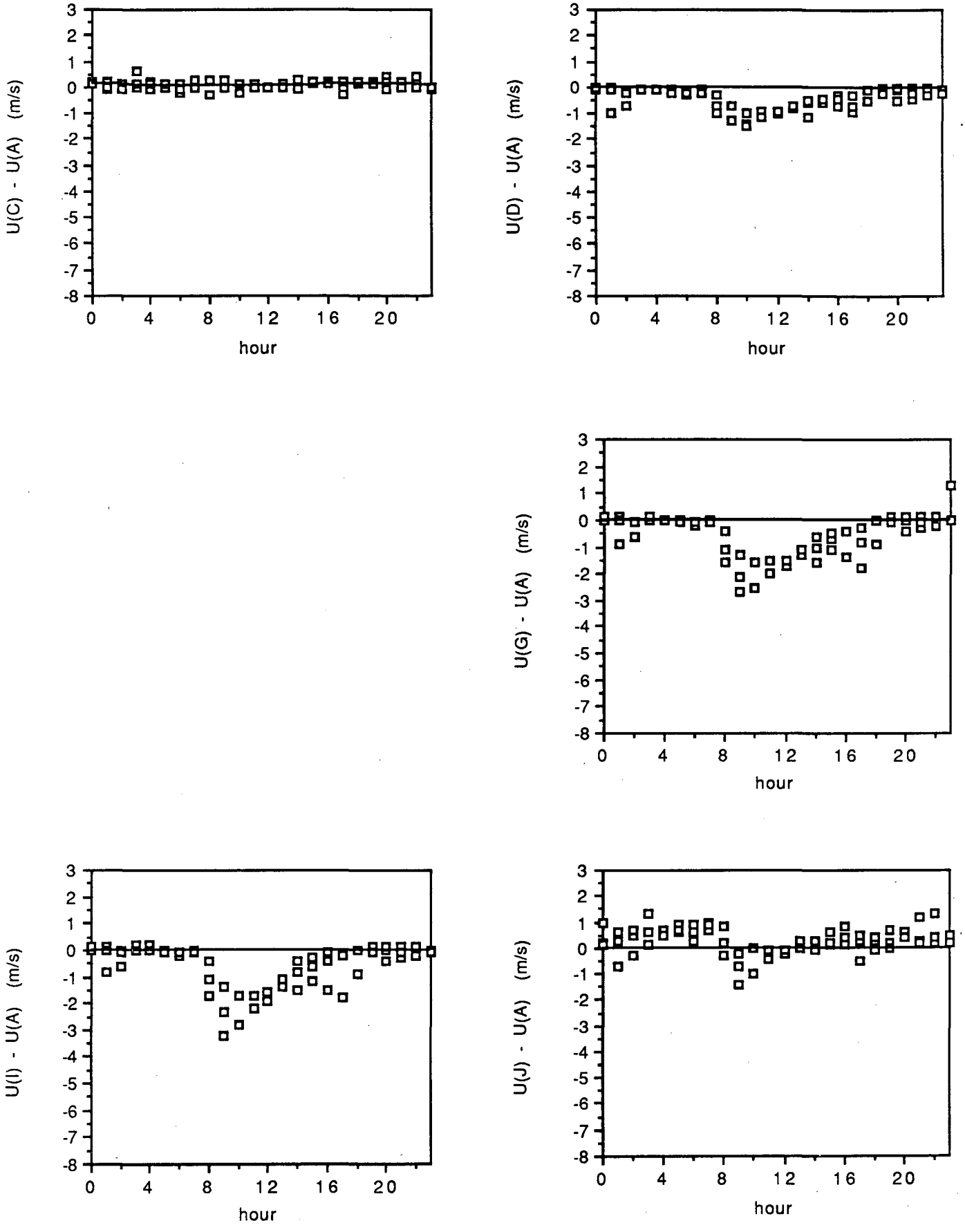

Figure 9. Clear day and night wind speed deviations from station A (m/s) for 3 days.

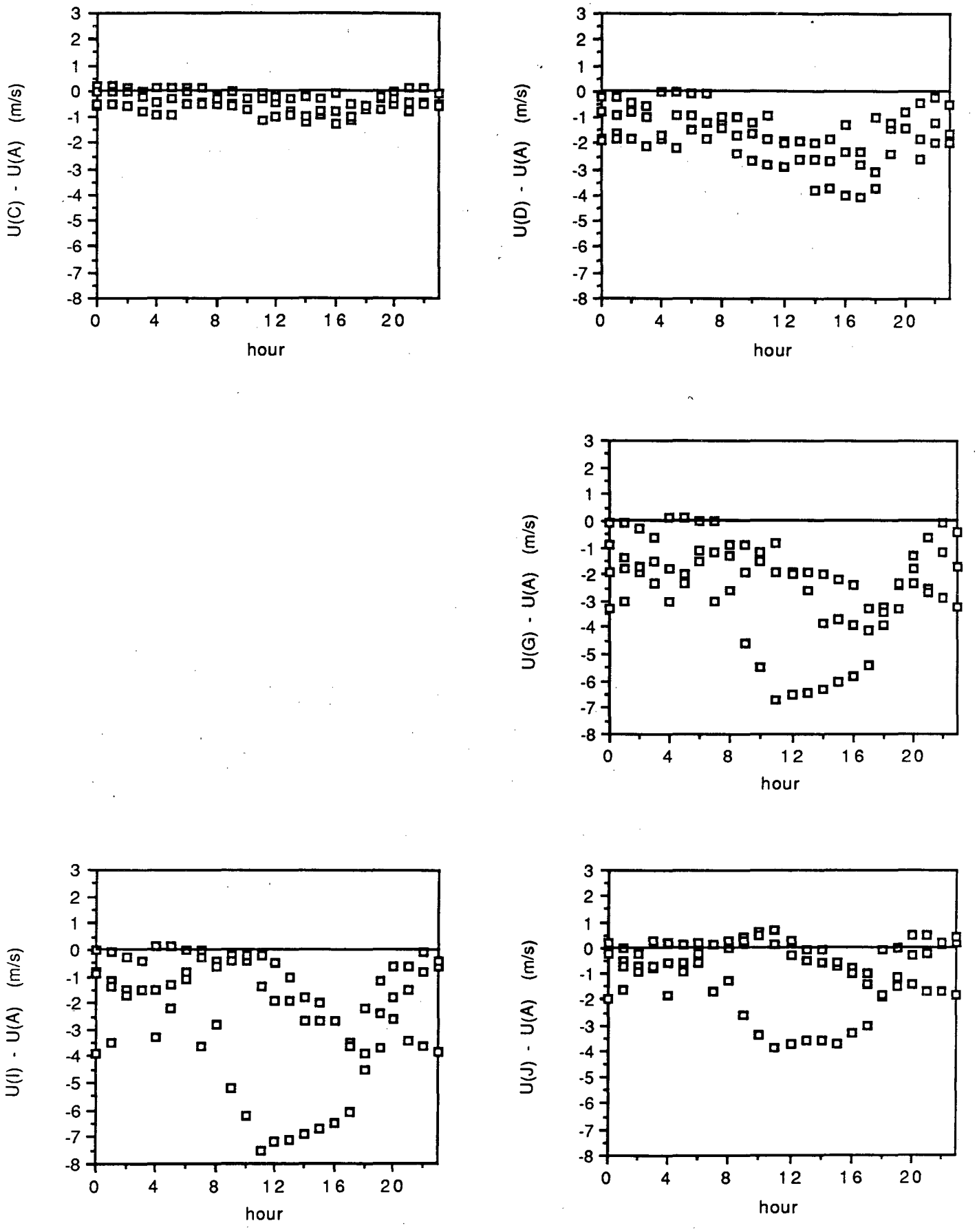

Figure 10. Overcast day and night wind speed deviations from station A (m/s) for 3 days.

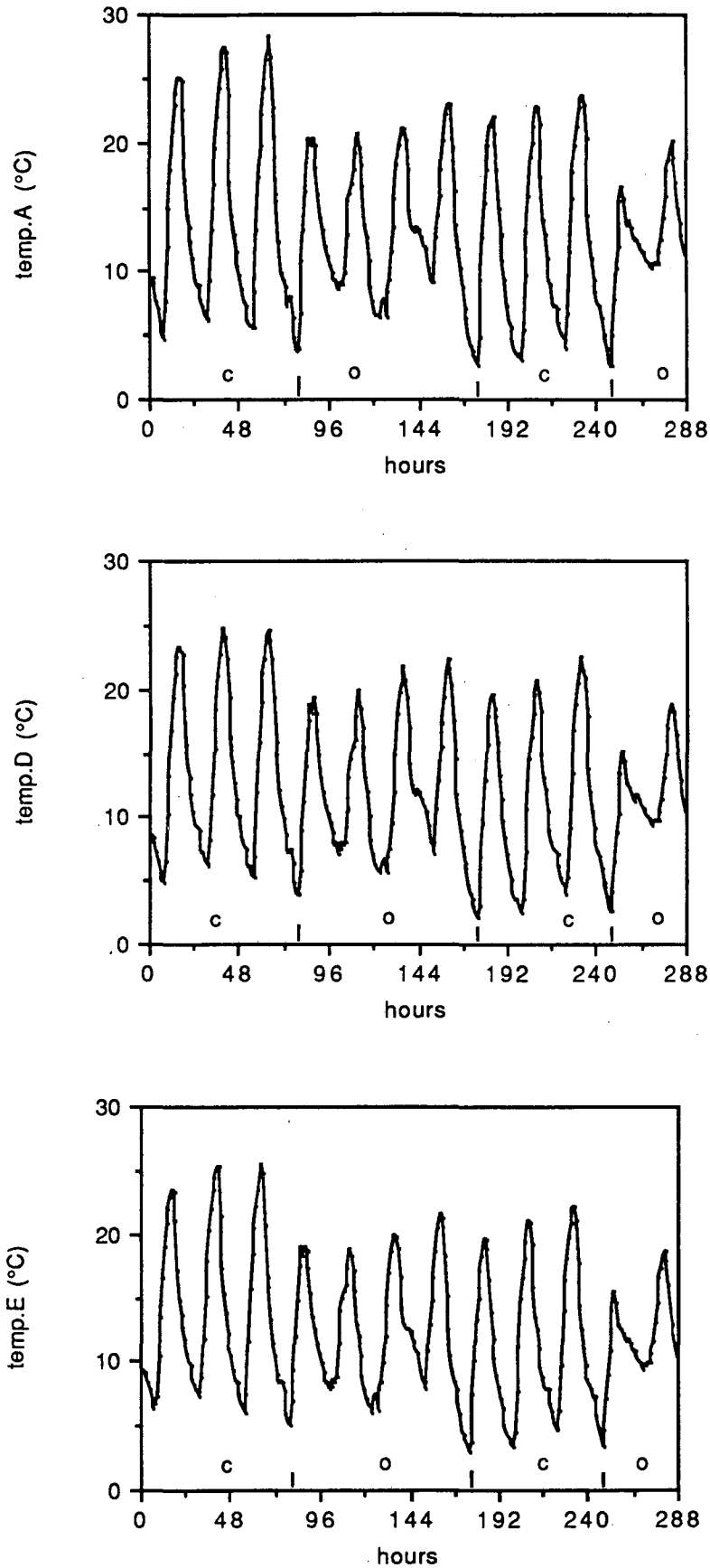

Figure 11. Overall temperatures (°C) during 12 days of the observational period. X-axis starts at hour 0:00 on October 13, 1986. (c=clear, o=overcast)

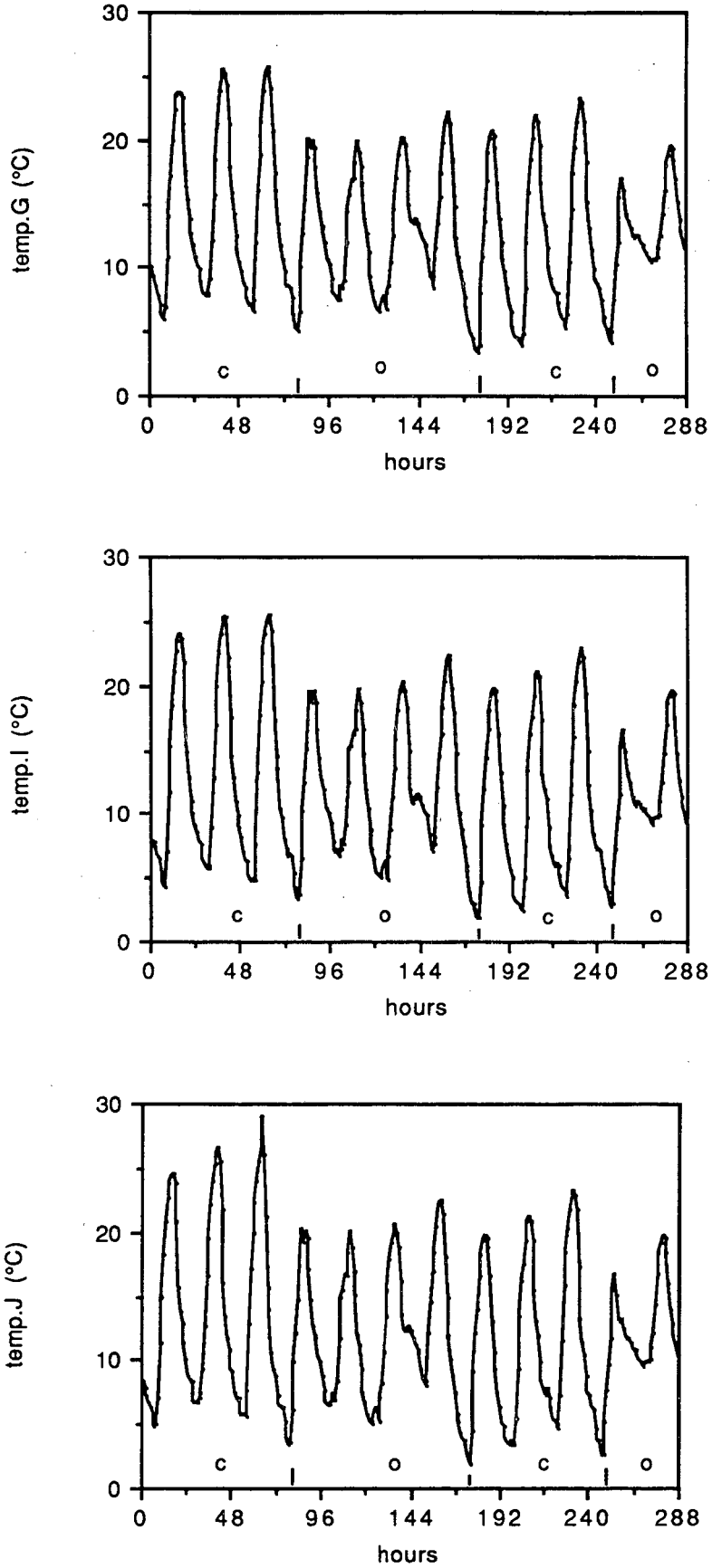

Figure 11 (cont'd). Overall temperatures (°C) during 12 days of the observational period. X-axis starts at hour 0:00 on October 13, 1986. (c=clear, o=overcast)

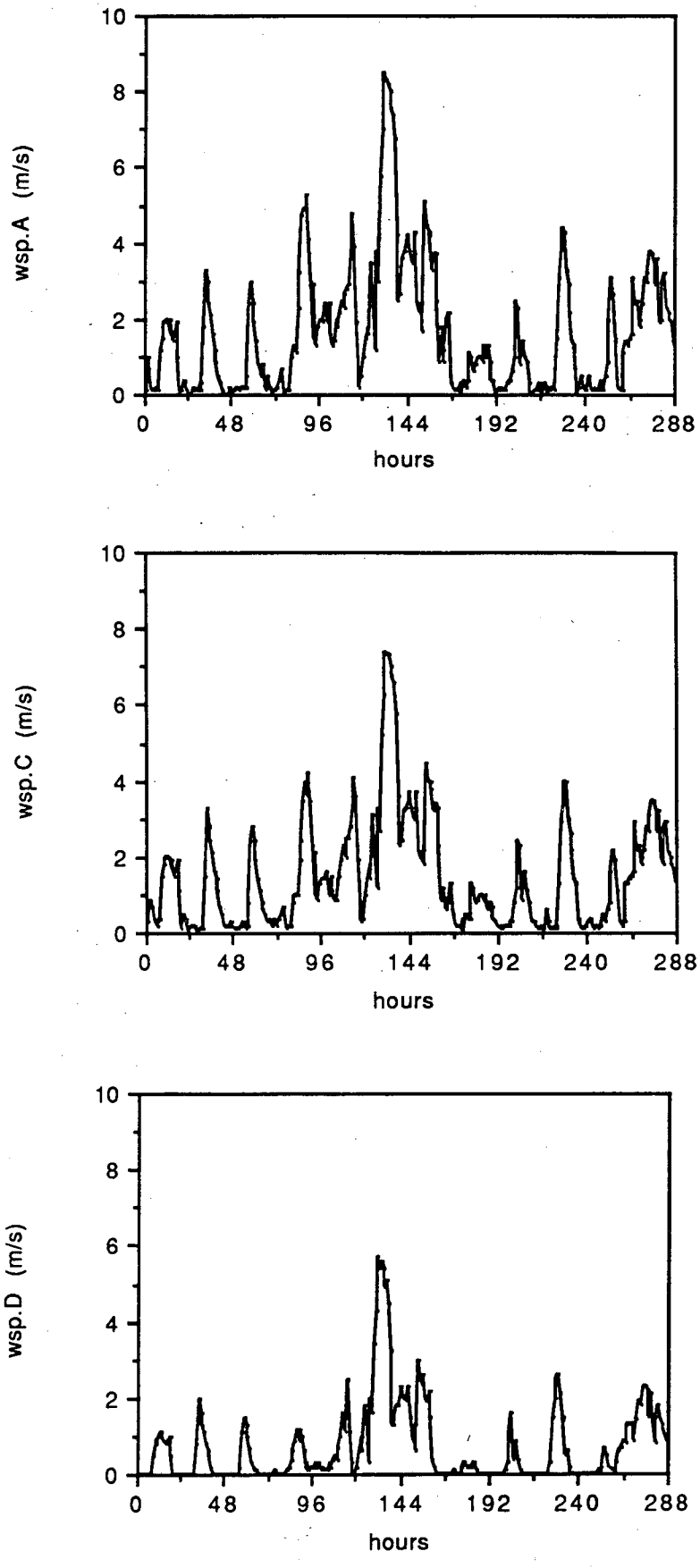

Figure 12. Overall wind speed (m/s) during 12 days of the observational period. X-axis starts at 0:00 hours on 13 October, 1986.

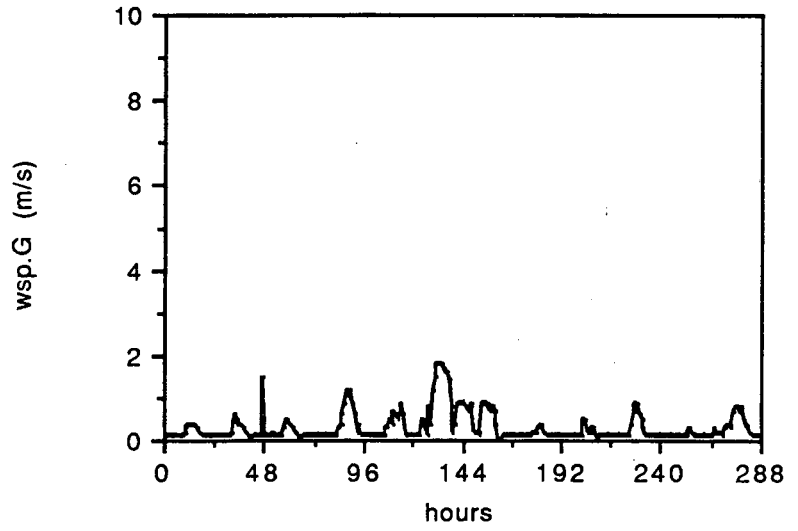

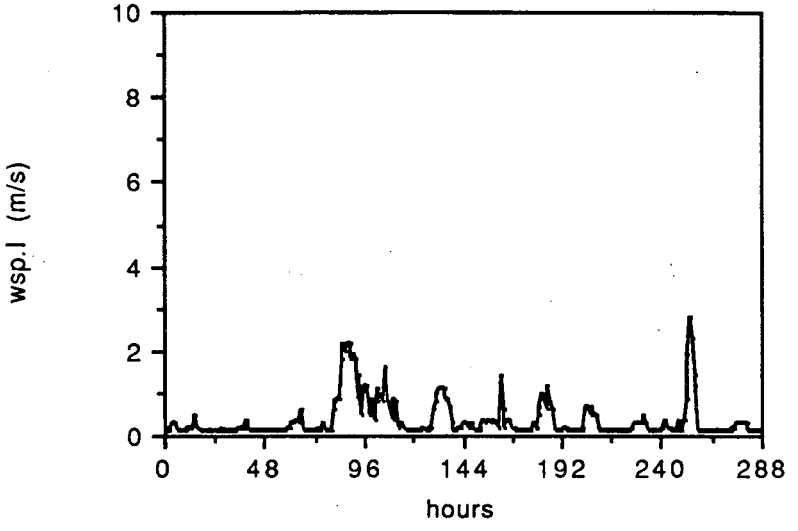

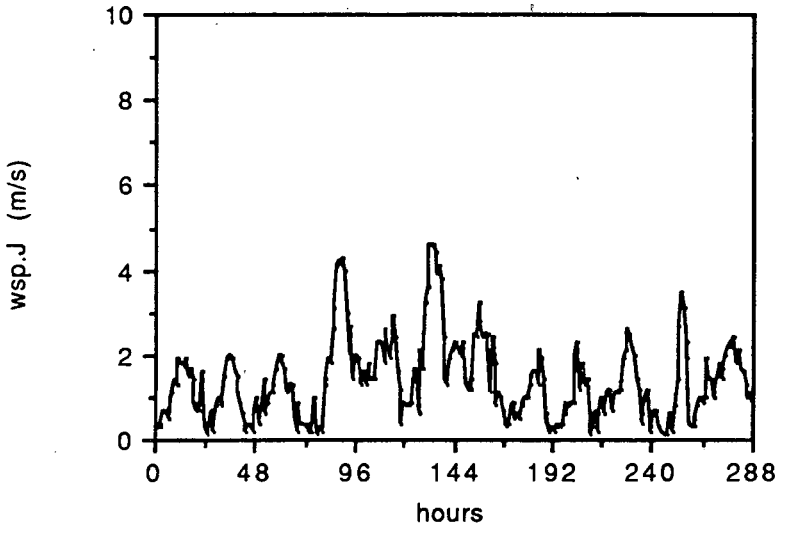

Figure 12 (cont'd). Overall wind speed (m/s) during 12 days of the observational period. X-axis starts at 0:00 hours on 13 October, 1986.

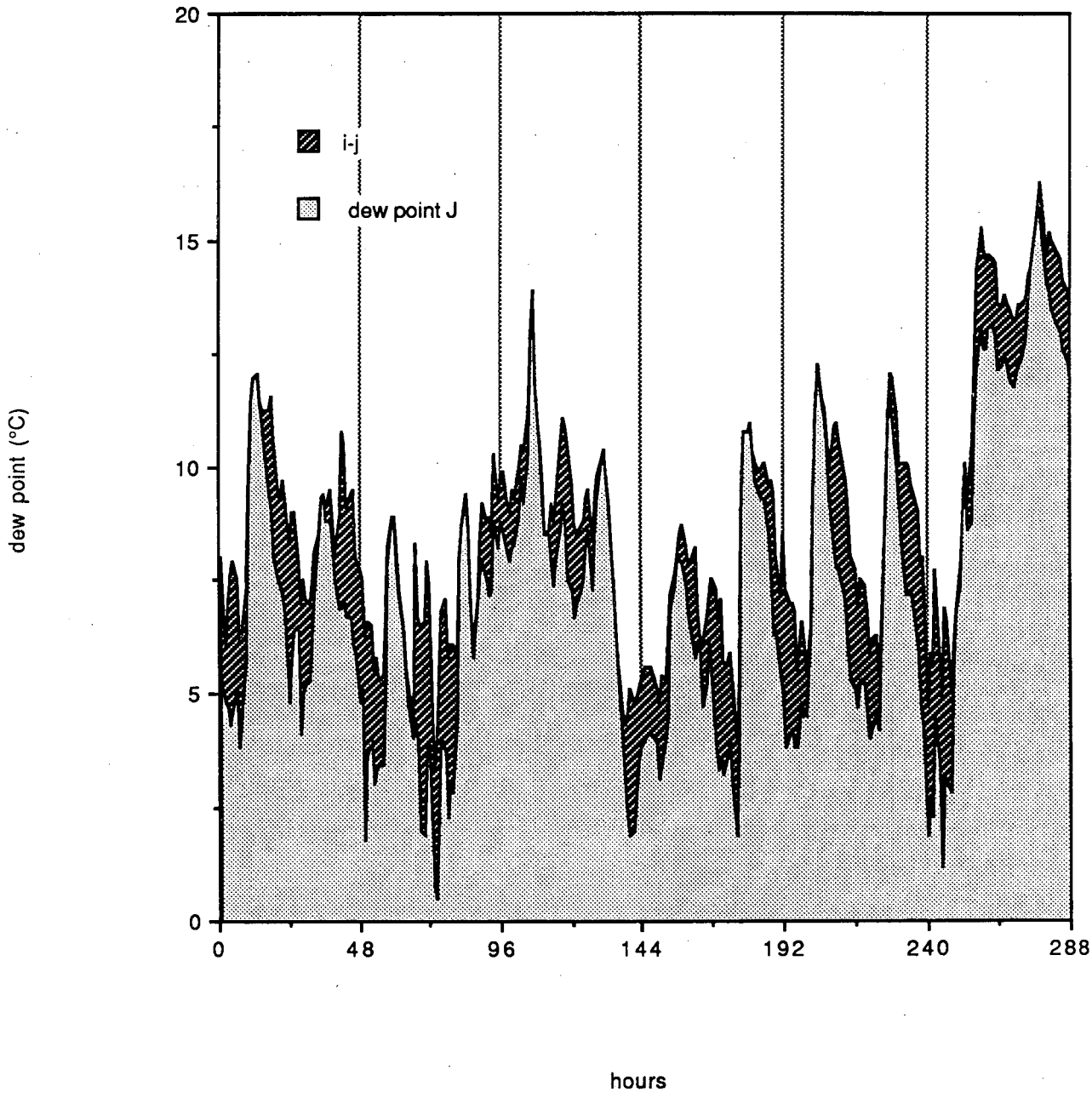

Figure 13. Dew point (°C) at stations I and J for 12 days during the observational period. X-axis starts at 0:00 hours on October 13, 1986.

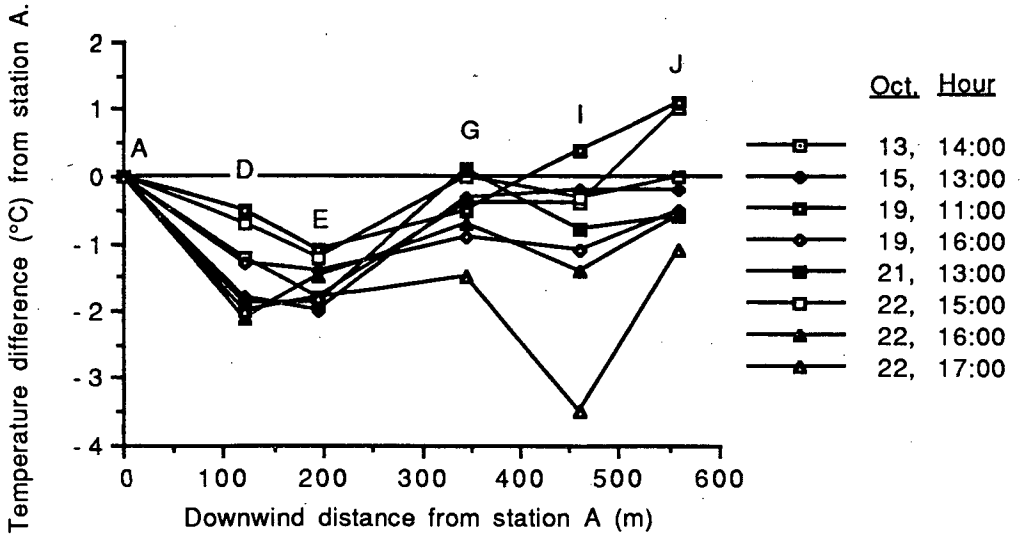

Figure 14. Temperature profiles across the canopy, for 8 hours with wind parallel to stations' line. (wind is blowing from north to south, i.e; from left to right)

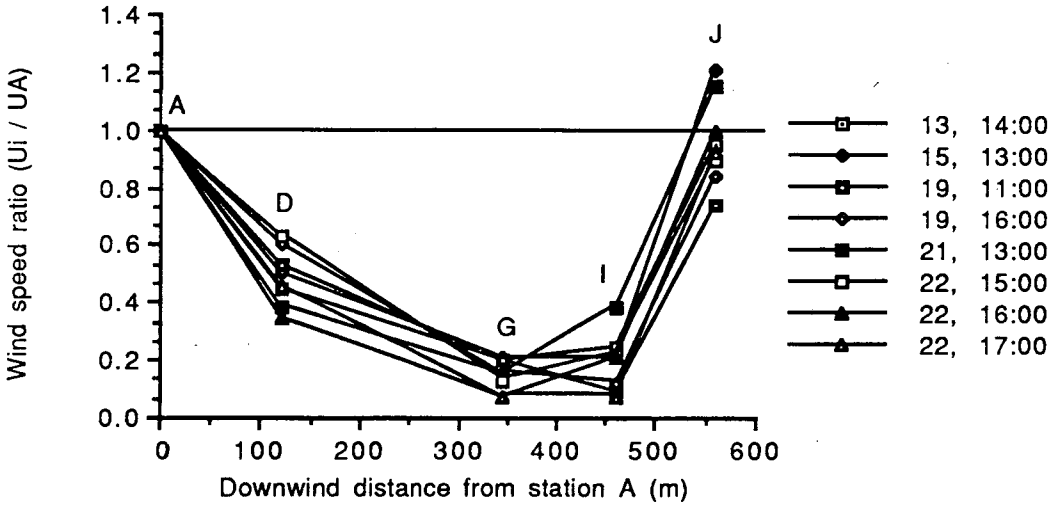

Figure 15. Wind Speed profiles across the canopy, for 8 hours with wind parallel to stations' line. (wind is blowing from north to south, i.e; from left to right)

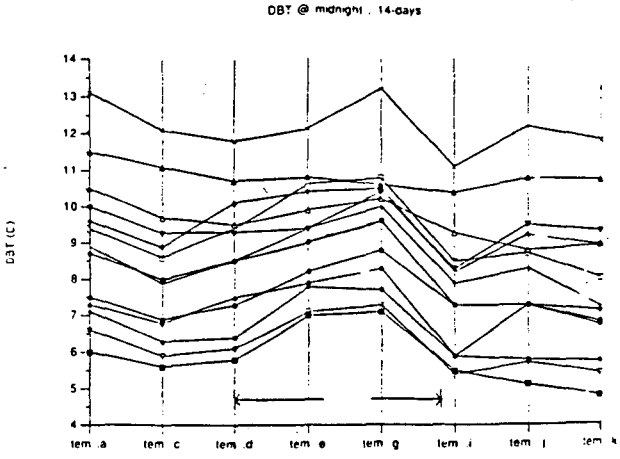

16

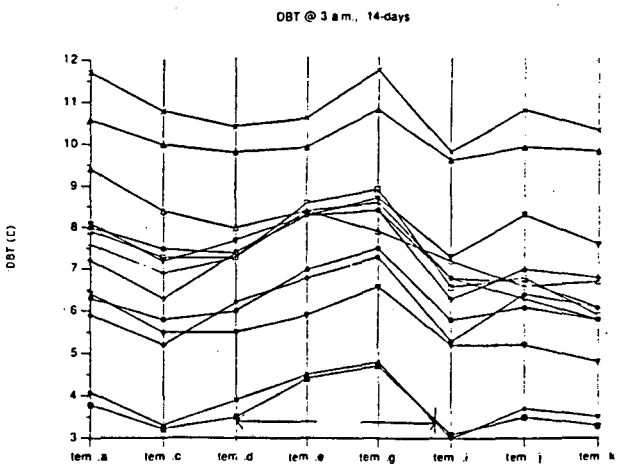

17

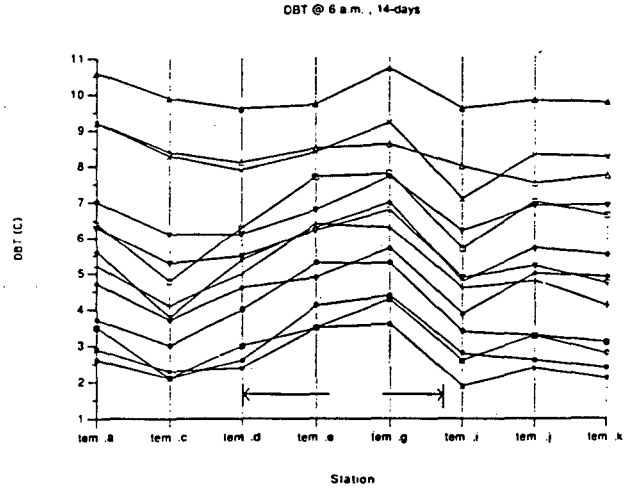

18

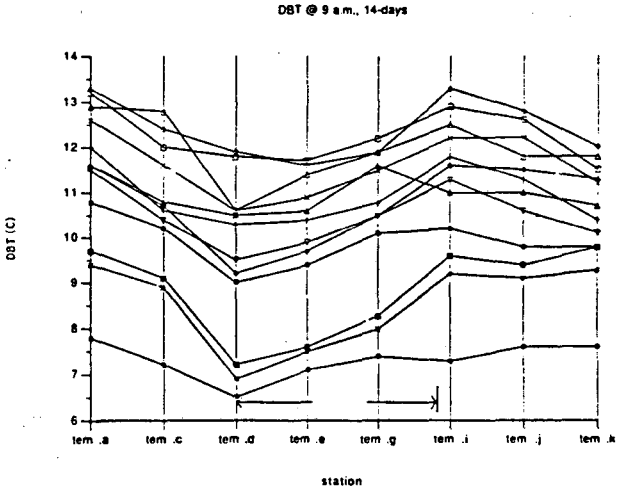

19

Figures 16-19.
Spatial and temporal evolution of the heat island and oasis effects.

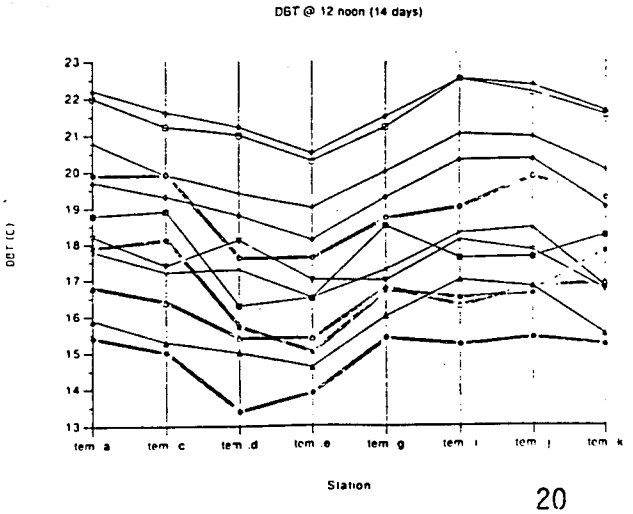

20

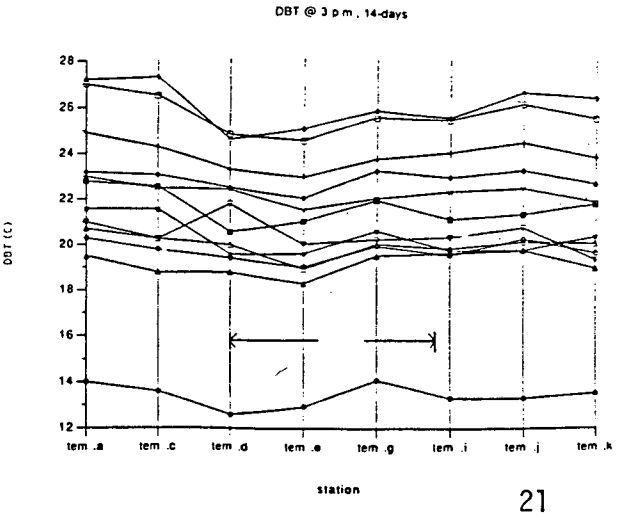

21

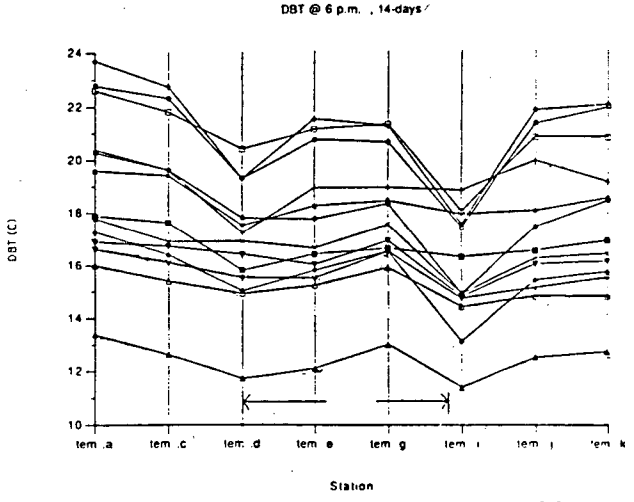

22

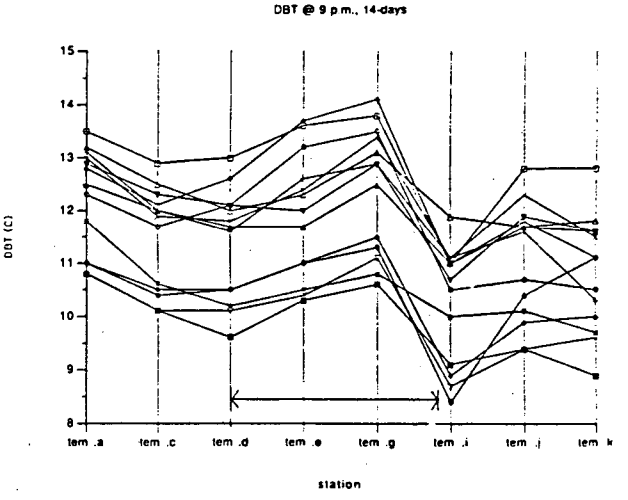

23

Figures 20-23.
Spatial and temporal evolution of the heat island and oasis effects.

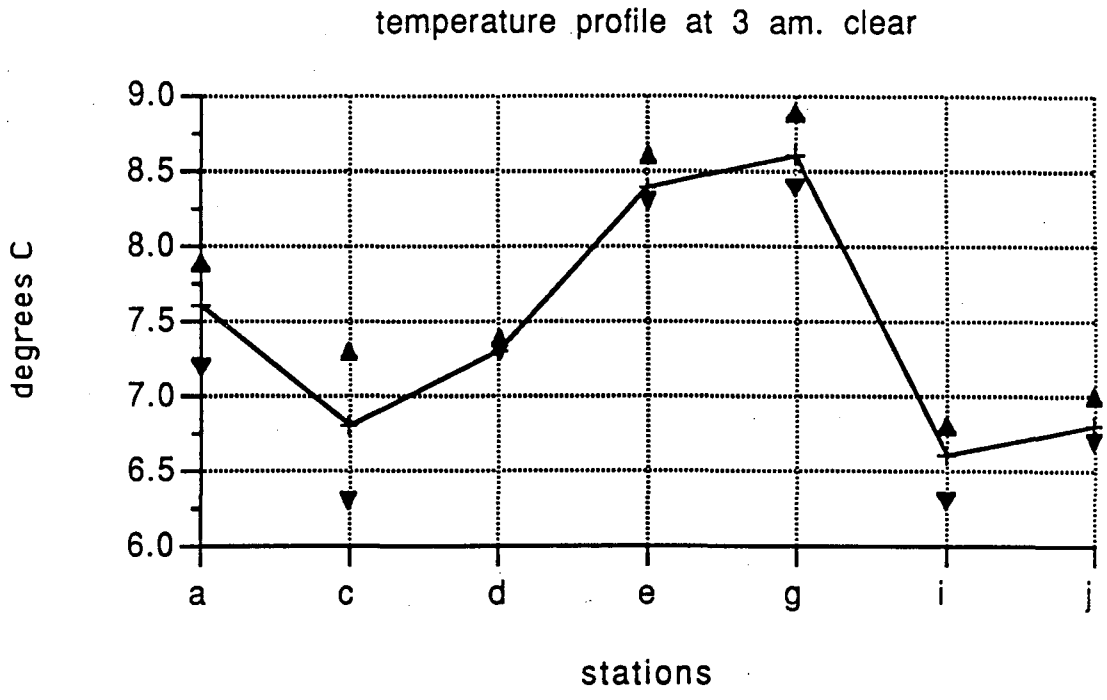

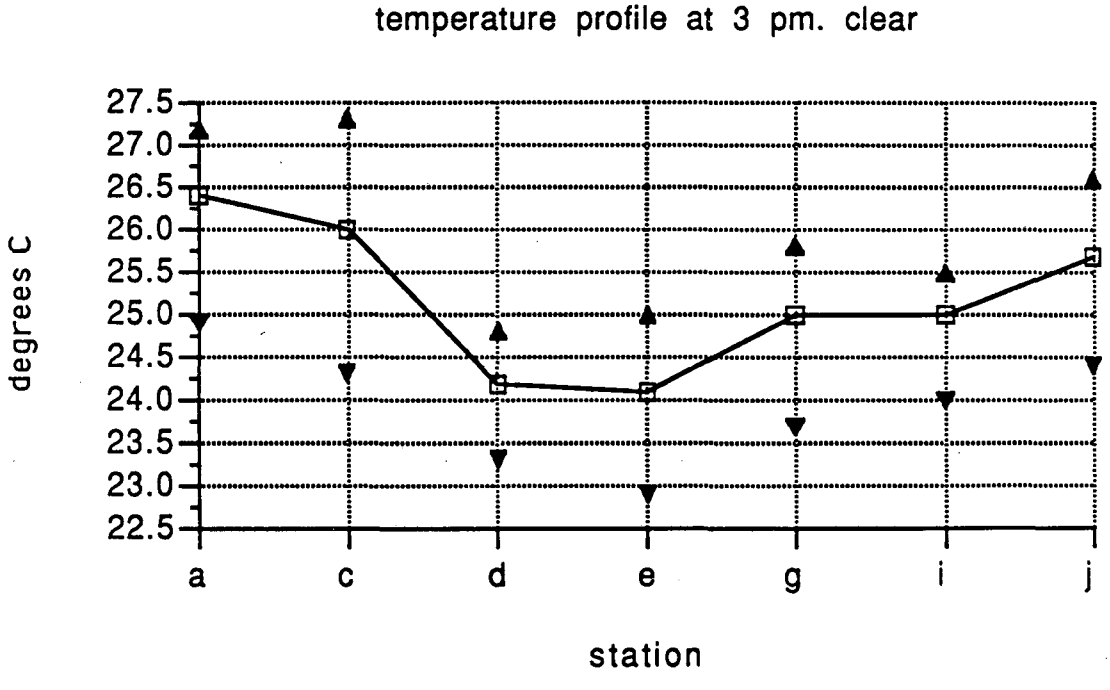

Figure 24.
Sample clear day snapshots at 3 am and 3 pm.

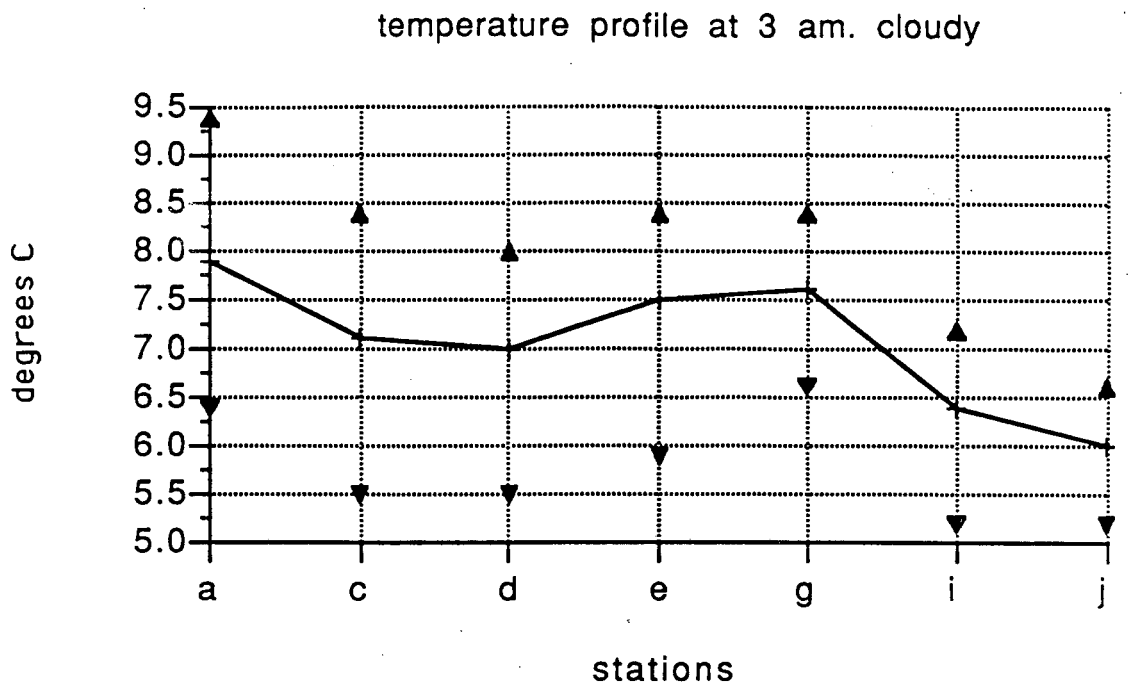

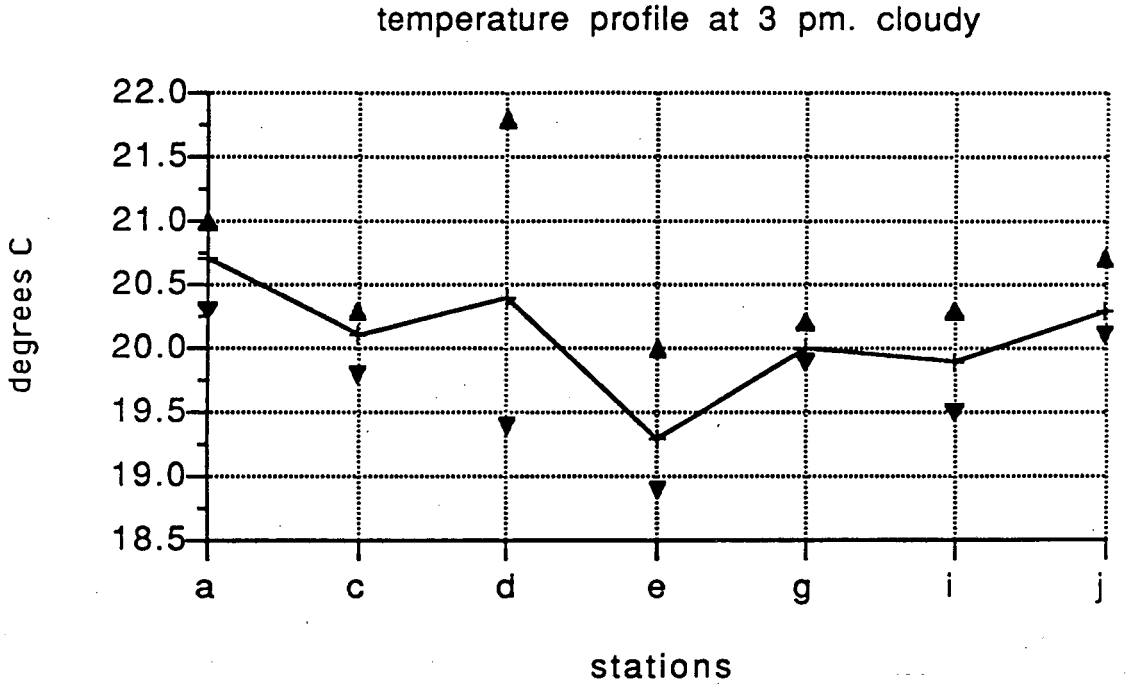

Figure 25.
Overcast day snapshots at 3 am and 3 pm.

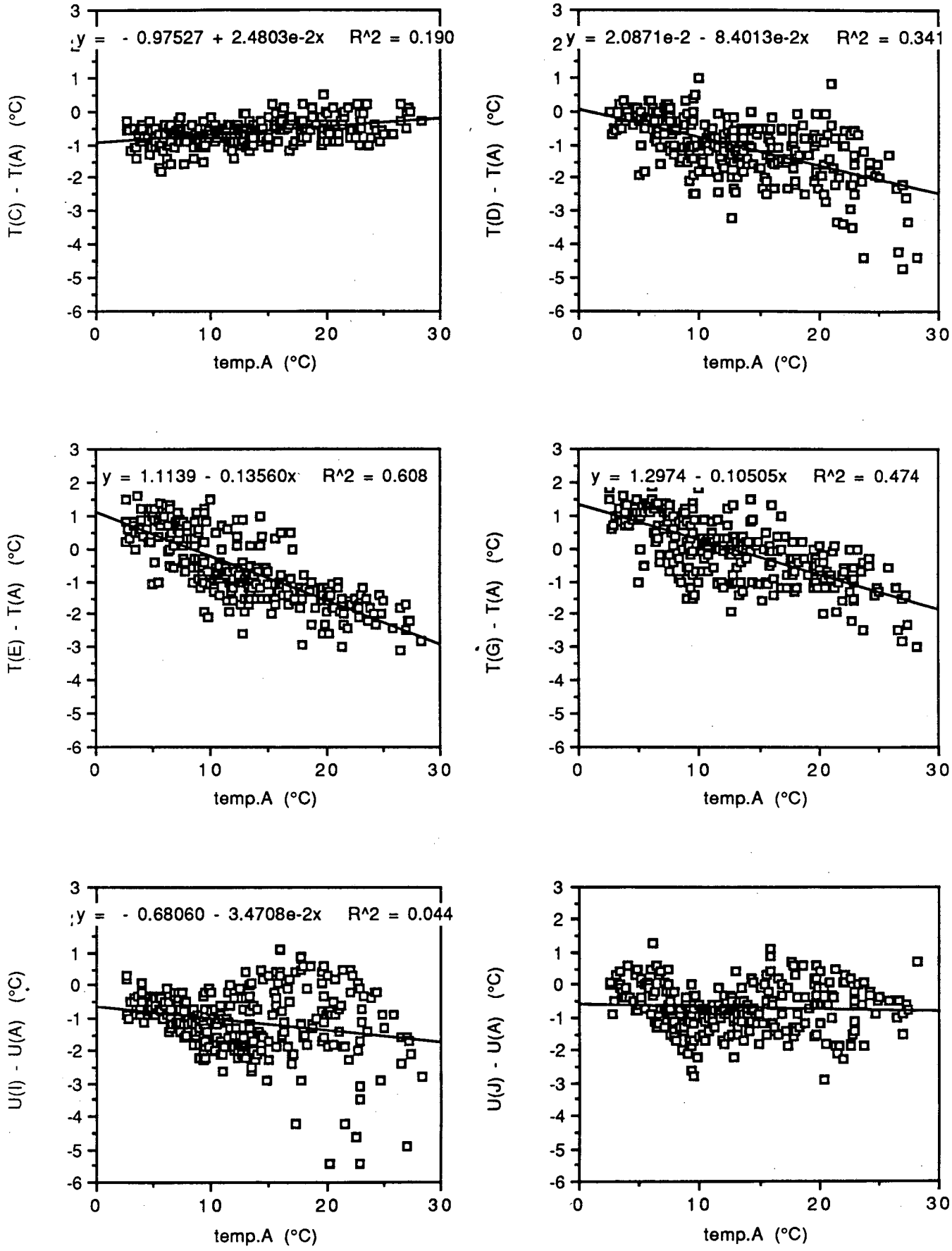

Figure 26. ΔT versus absolute temperature at all times.
Includes day/night and clear/overcast conditions.

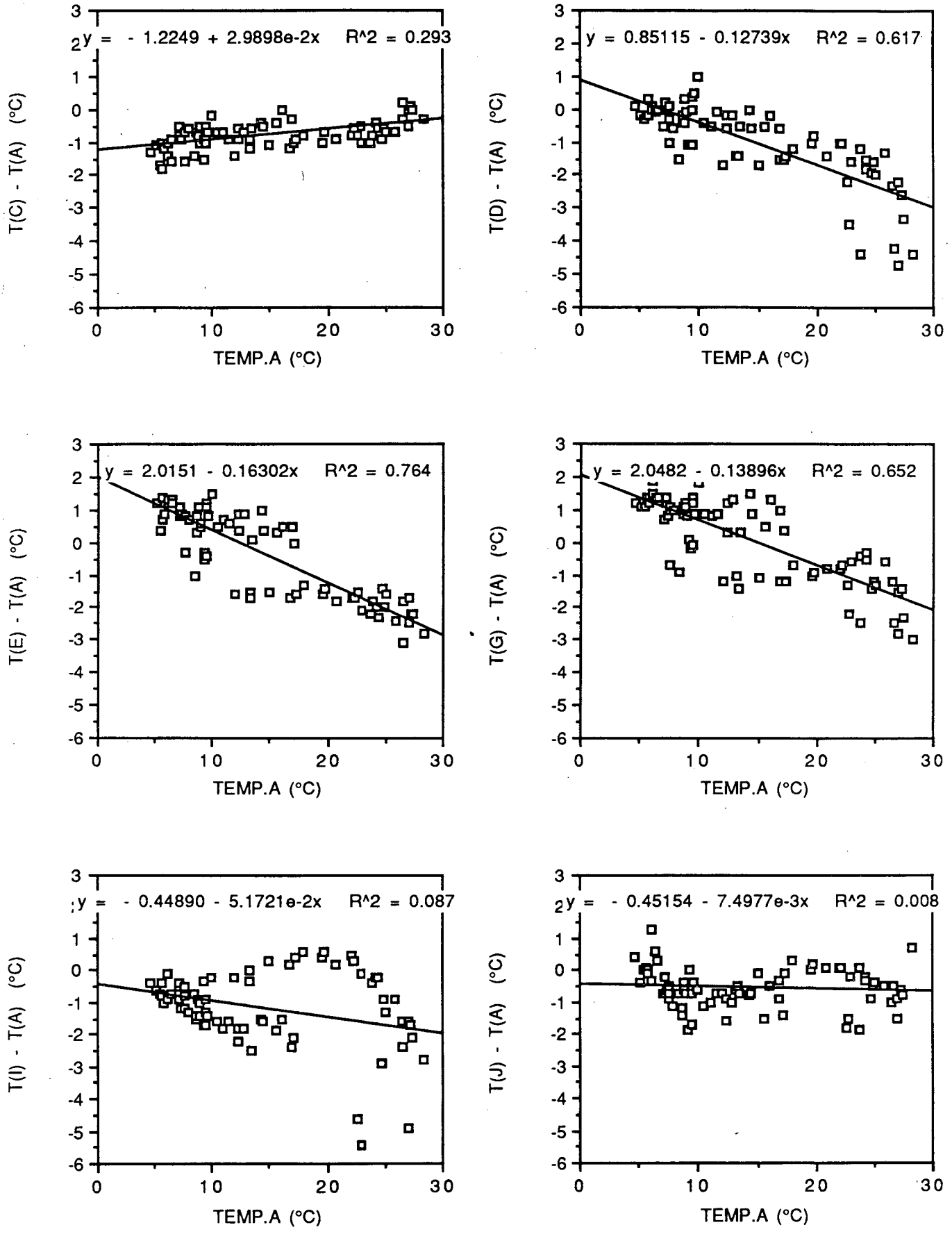

Figure 27. ΔT versus absolute temperature during clear days and nights.

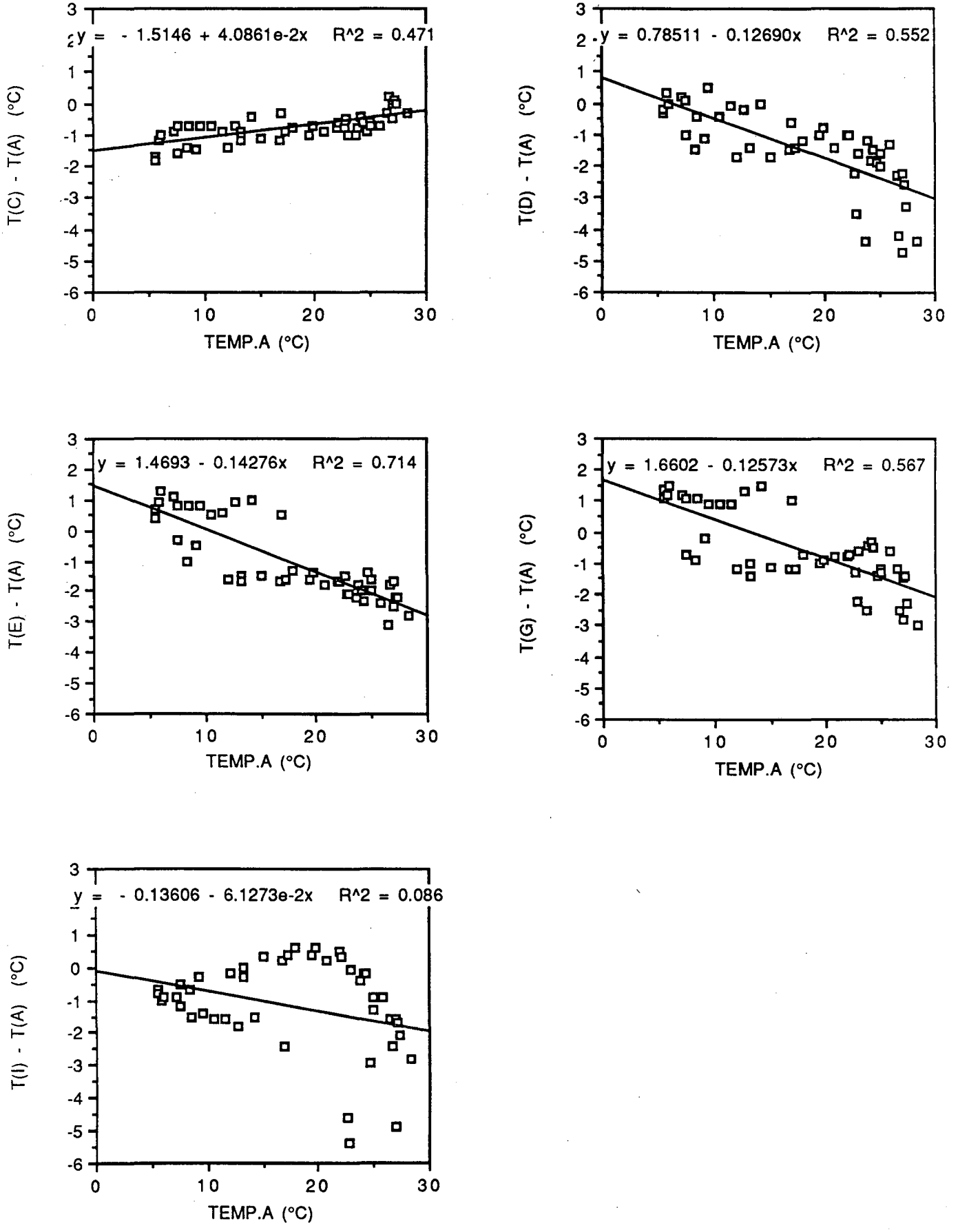

Figure 28. ΔT versus absolute temperature during clear daylight hours.

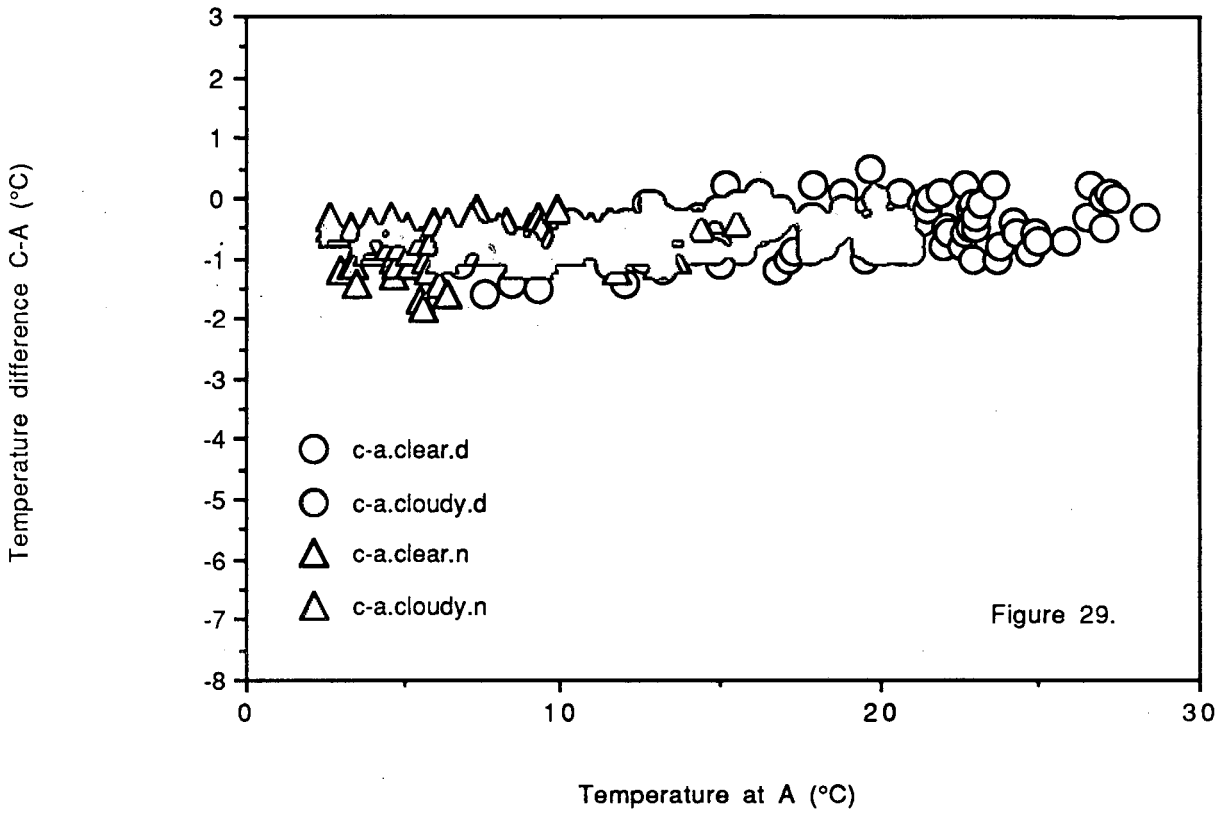

Figure 29.

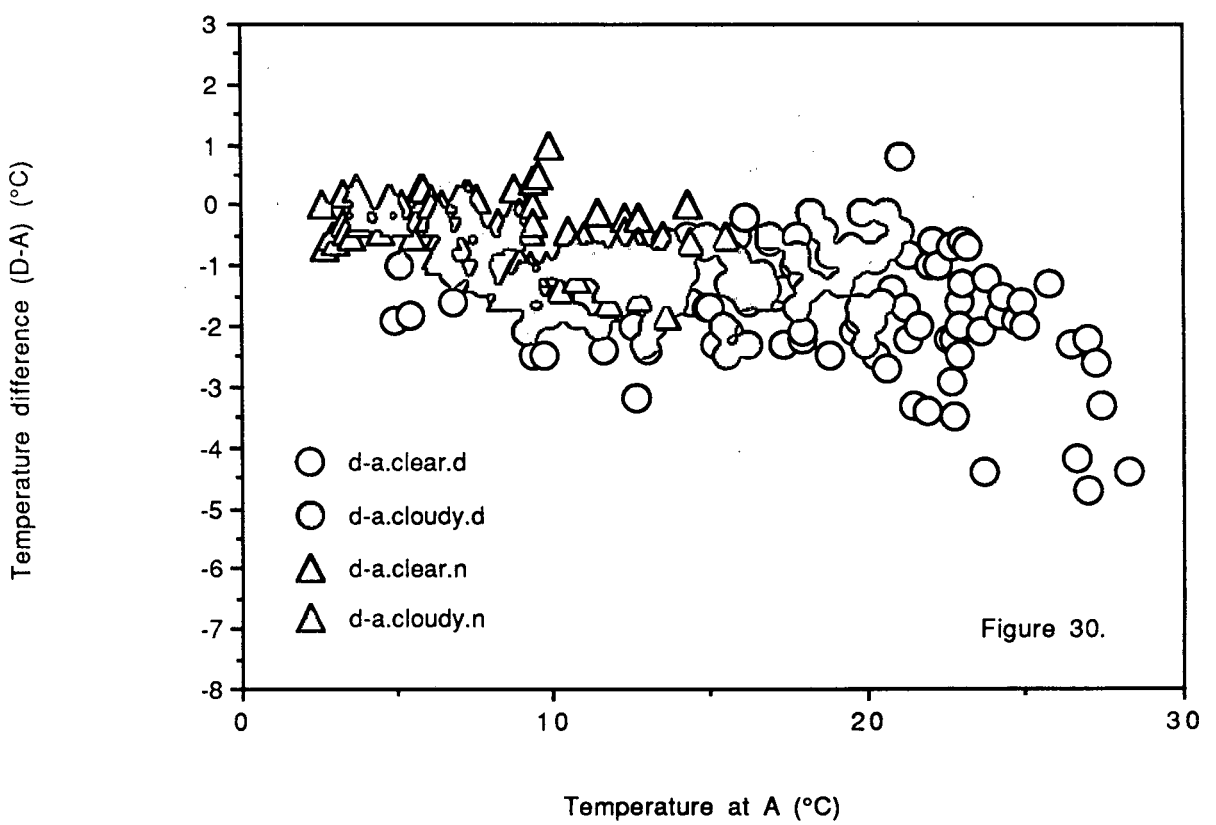

Figure 30.

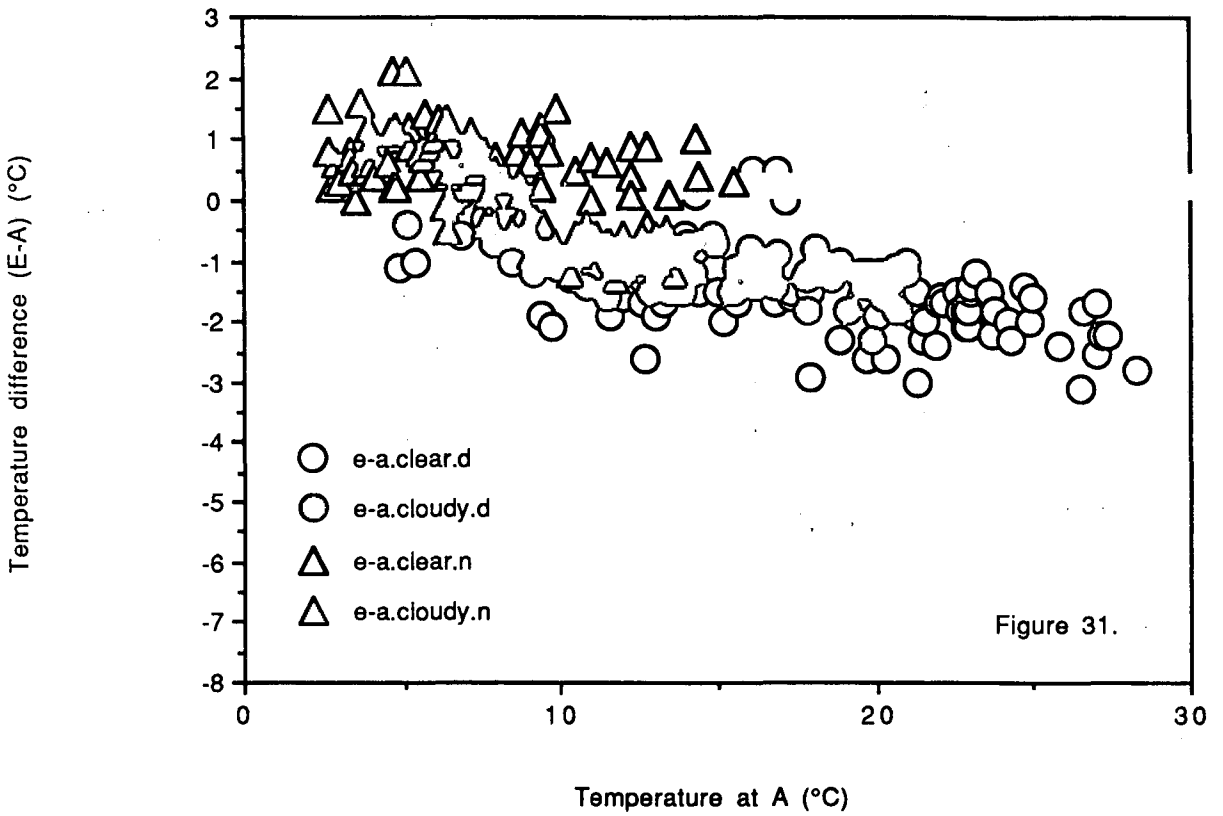

Figure 31.

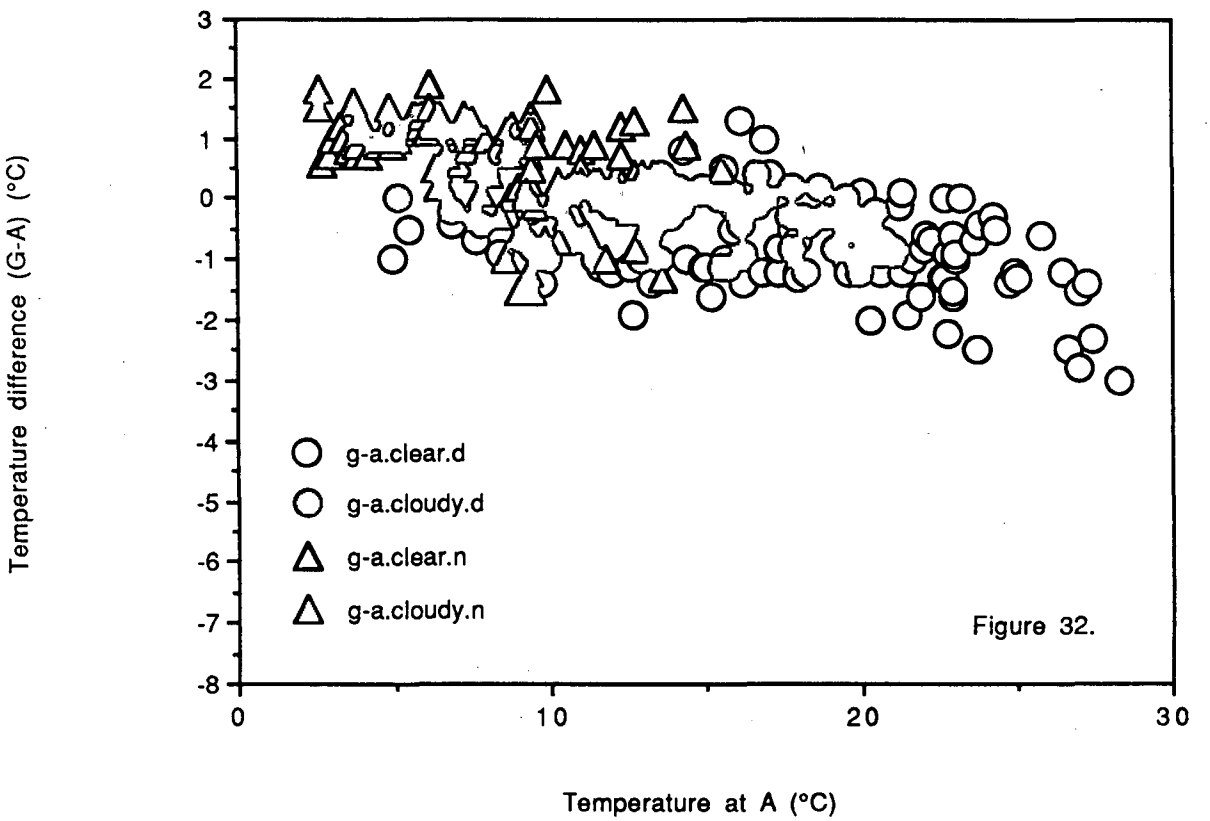

Figure 32.

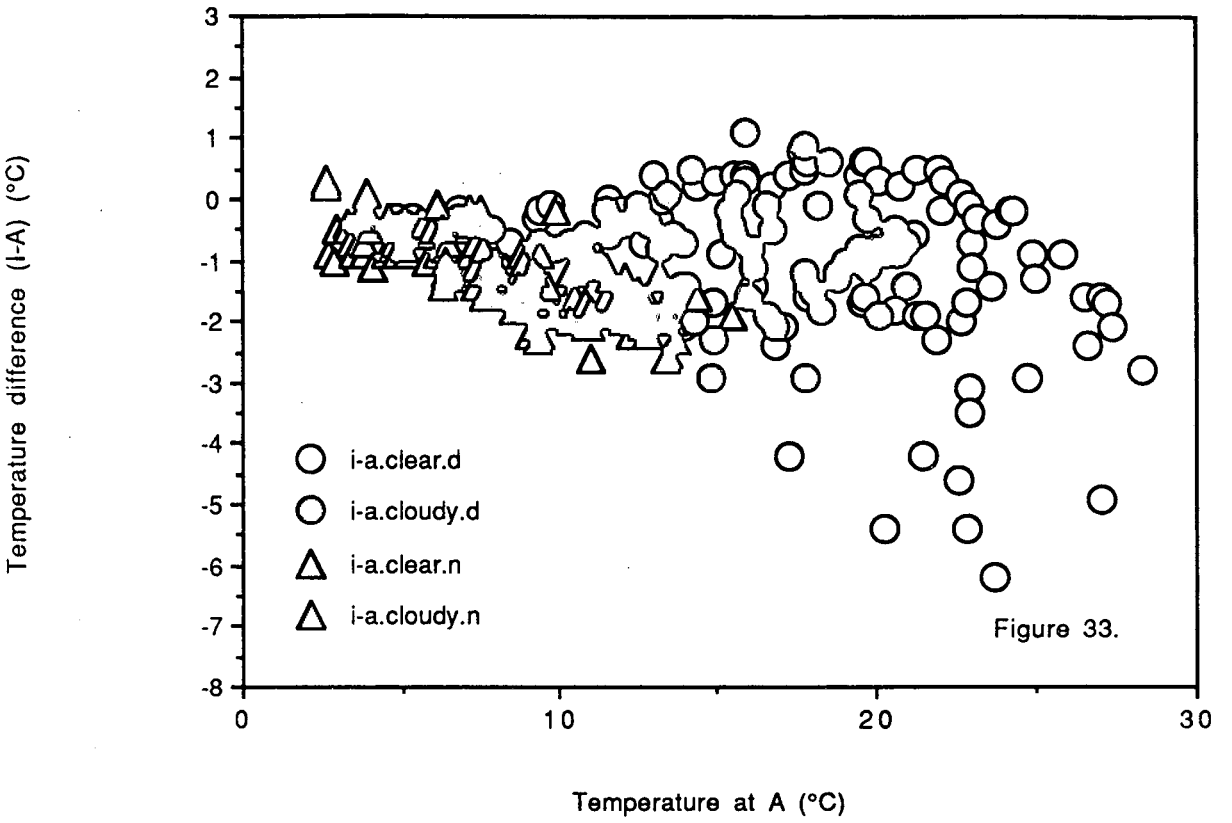

Figure 33.

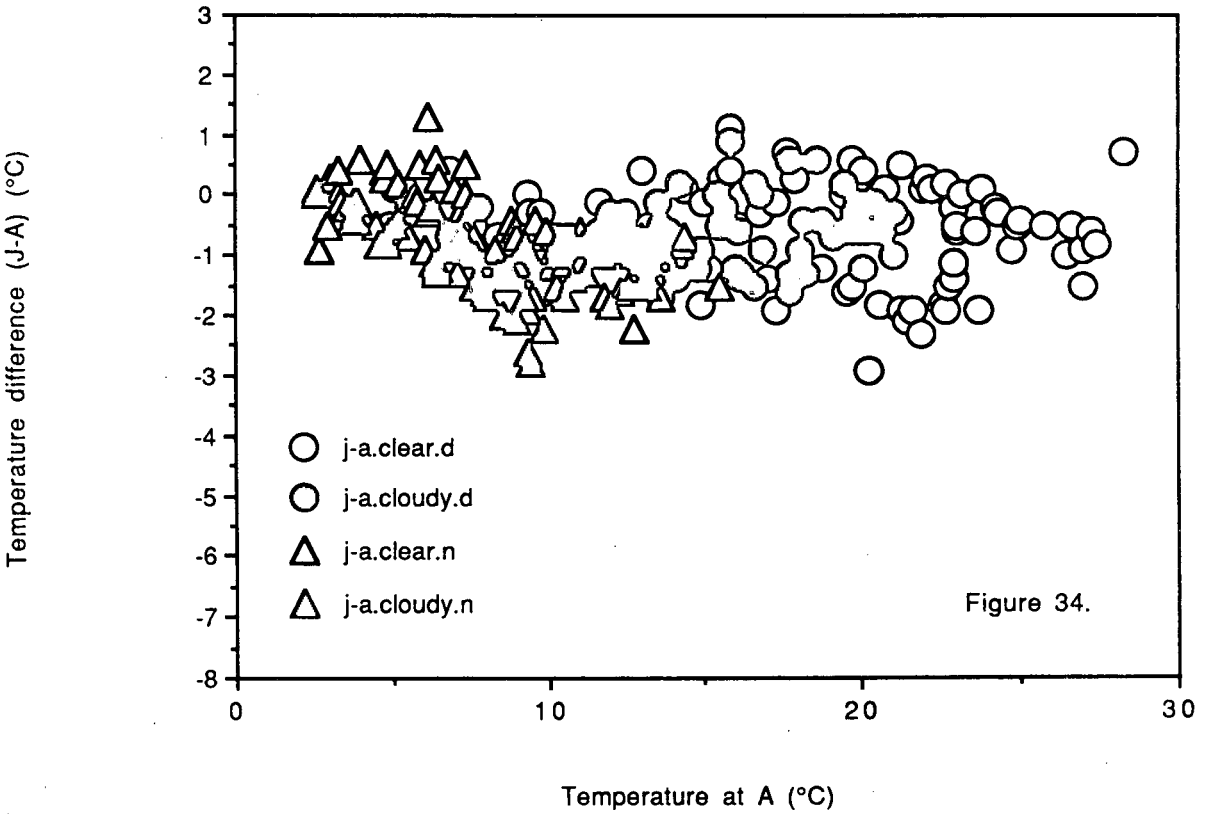

Figure 34.

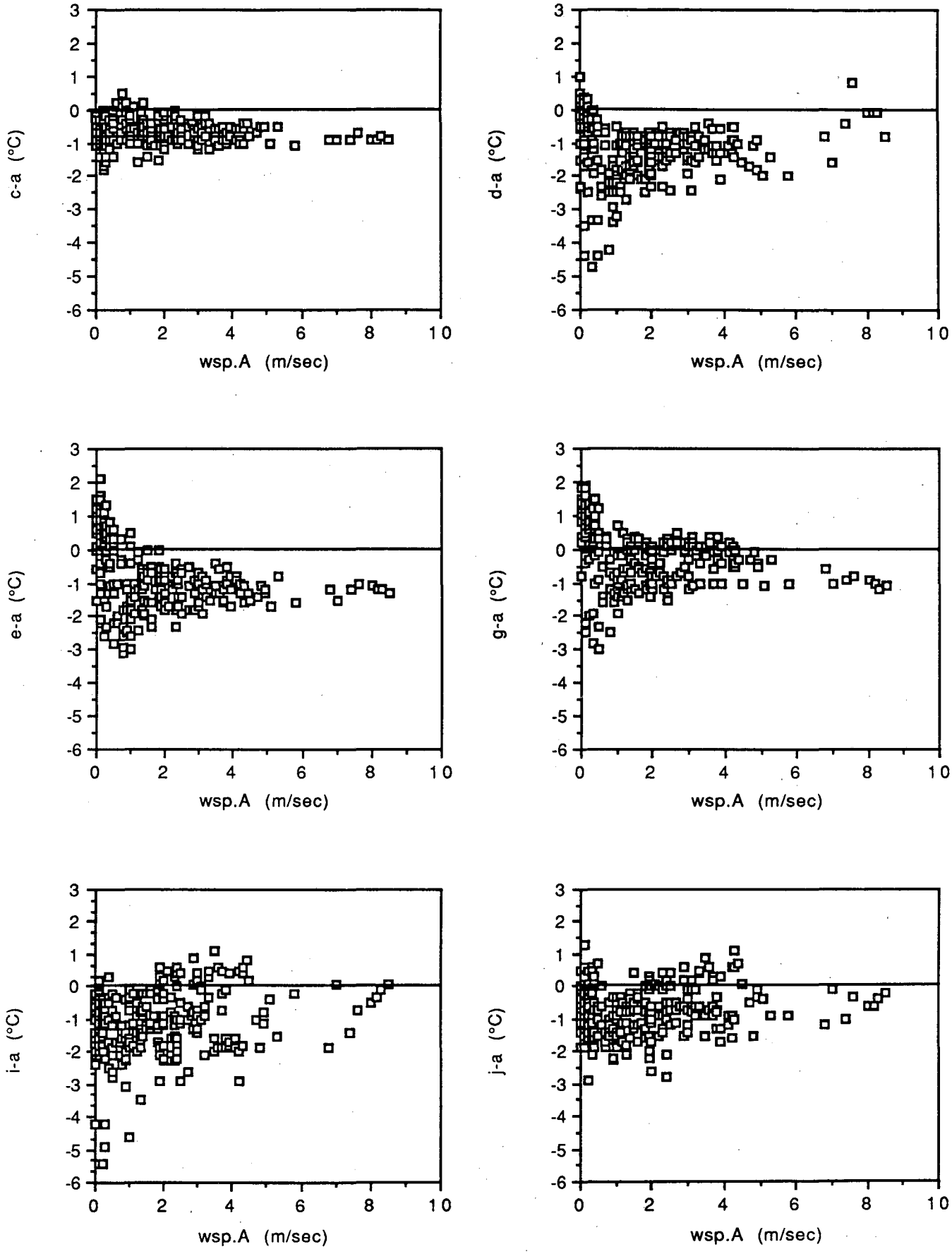

Figure 35. ΔT (°C) versus wind speed (m/s) for all times. Control station is location A.

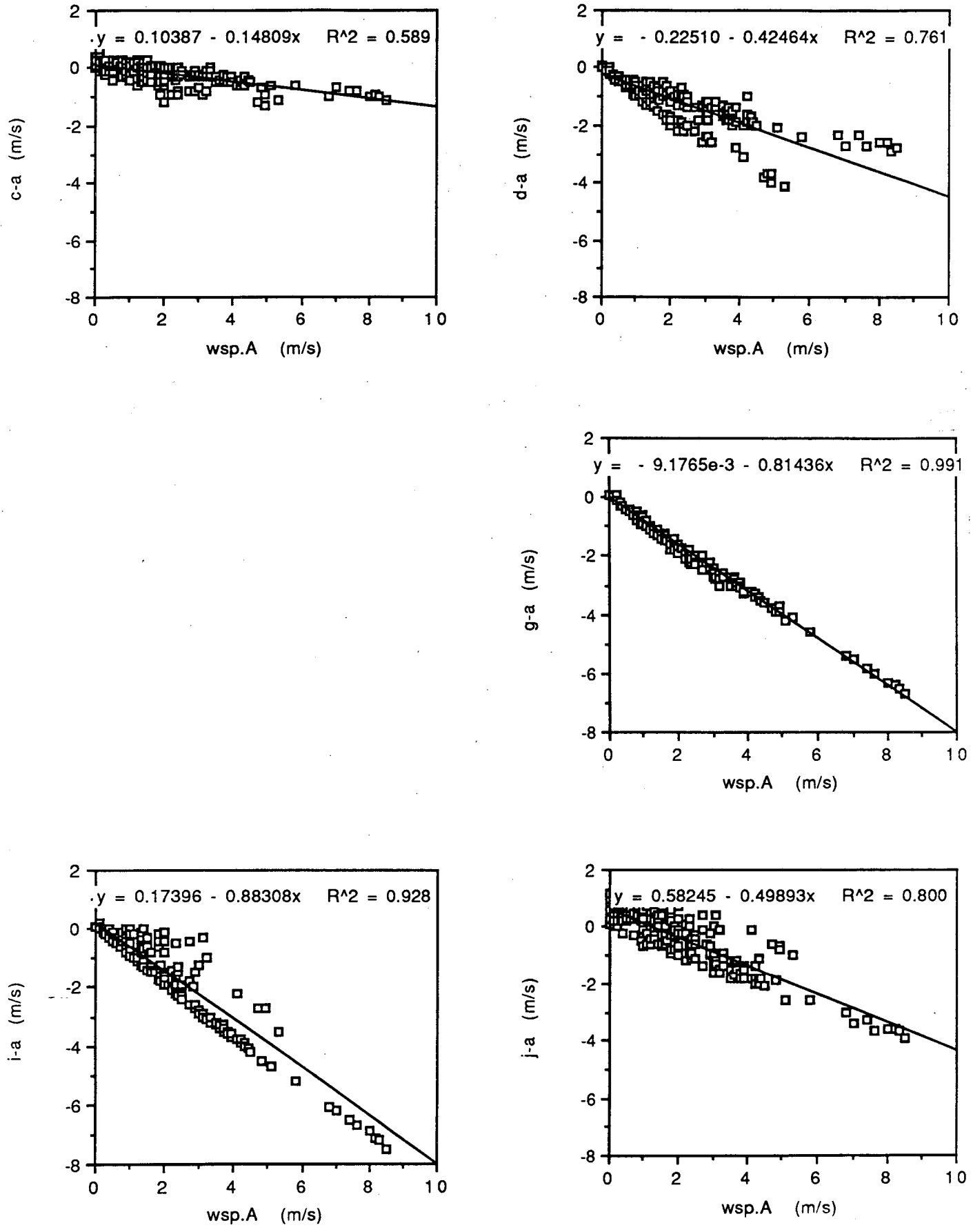

Figure 36. ΔV (m/s) versus absolute wind speed (m/s) for all times.

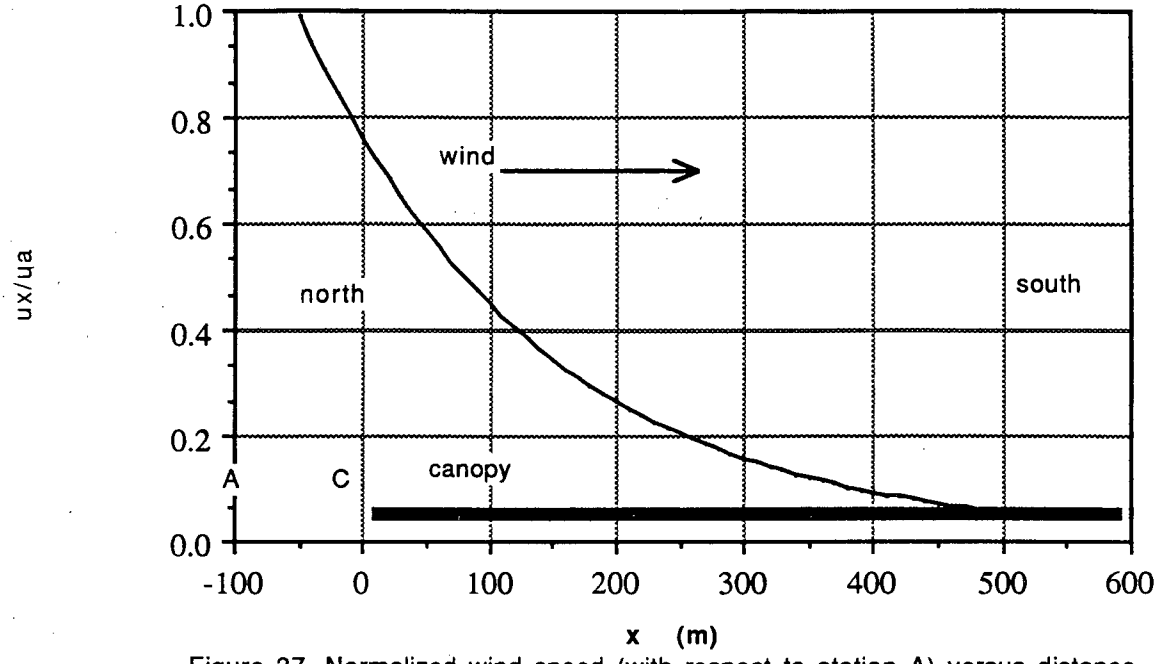

Figure 37. Normalized wind speed (with respect to station A) versus distance from the leading edge of the canopy, for wind from N ± 30°. (Decelerating case).

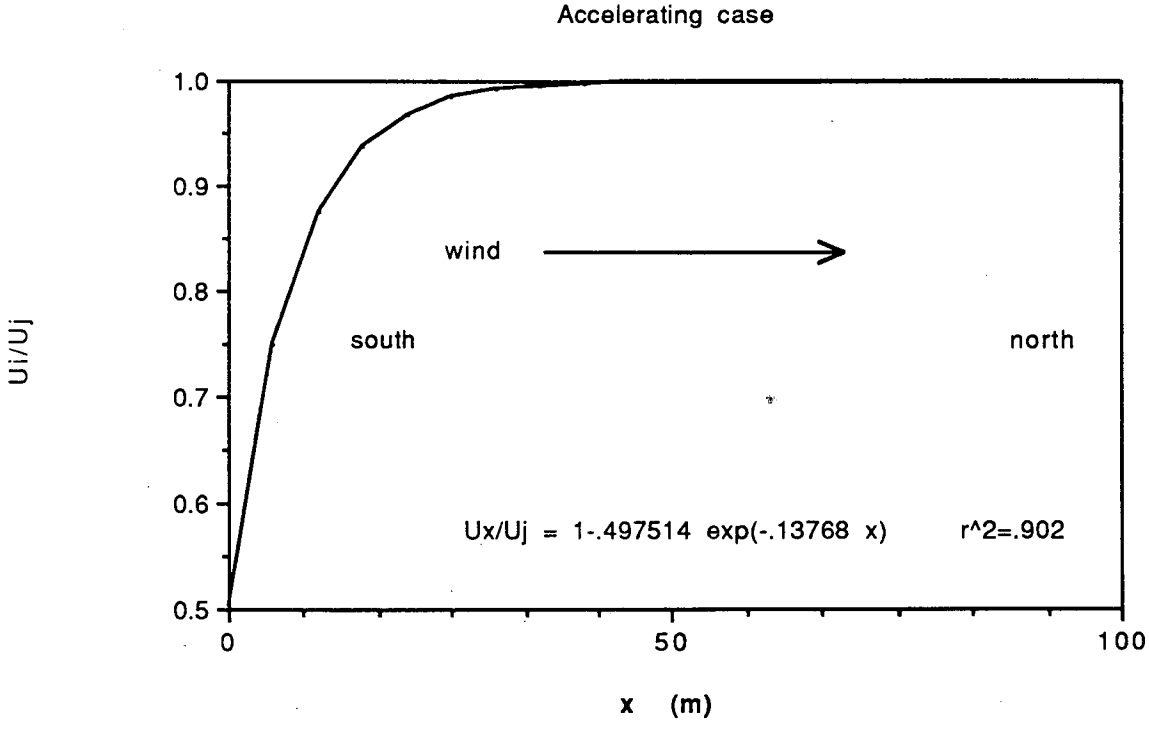

Figure 38. Normalized wind speed (with respect to station J) versus distance from canopy, for wind from S ± 30°. (Accelerating case).

LAWRENCE BERKELEY LABORATORY
UNIVERSITY OF CALIFORNIA
INFORMATION RESOURCES DEPARTMENT
BERKELEY, CALIFORNIA 94720